On the role of surface properties for implant fixation

From finite element modeling to in vivo studies

Patrik Stenlund

Department of Biomaterials
Institute of Clinical Sciences
Sahlgrenska Academy at University of Gothenburg

UNIVERSITY OF GOTHENBURG

Gothenburg 2015

Cover illustration: A finite element model and an implant screw highlighting the bone-implant interface and the surface topography visualized by 3D-SEM.

On the role of surface properties for implant fixation

patrik.stenlund@sp.se

ISBN 978-91-628-9380-4
http://hdl.handle.net/2077/38371

Printed in Gothenburg, Sweden 2015
Ineko AB

Till Ellinor & Janne

ABSTRACT

The aim of this thesis was to gain a deeper understanding of the factors contributing to the fixation of bone-anchored implants, especially with regard to surface chemistry, surface topography and implant loading. The methodology used in the thesis ranges from systematic bench studies, computer simulations, experimental *in vivo* studies, to load cell measurements on patients treated with bone-anchored amputation prostheses.

The bone response to the surface chemistry was the main factor of interest in paper I and II. It was evaluated by adding a low amount of Zr to electron beam melted Co–Cr–Mo implants *in vivo* using a rabbit model, and a novel Ti–Ta–Nb–Zr alloy was compared to cp–Ti *in vivo* using a rat model, respectively. Surface roughness parameters and factors related to the removal torque technique were identified in a systematic experimental study (Paper III). Finite element analysis was used to study the effect of surface topography and geometry on mechanical retention and fracture progression at the implant interface (Paper IV). In the last paper, site-specific loading of the bone-implant interface was measured on patients treated with bone-anchored amputation prosthesis. The effect of typical every-day loading for the bone-implant system was simulated by finite element analysis. Evaluation of retrieved tissue samples from a patient undergoing implant revision was conducted to determine the interfacial condition after long-term usage (Paper V).

It was concluded that the surface topography, the surface chemistry and the medium surrounding the implant were all found to influence the stability of the implant. A model of interfacial retention and fracture progression around an implant was proposed. Observations of bone resorption around an amputation abutment can partly be explained by the long-term effect of daily loading.

In summary, the implant surface properties can be tailored for improved biomechanical anchorage and optimal load transfer, thus reducing the risk of implant failures and complications in patients.

SAMMANFATTNING

Infästning av proteser görs bland annat med benförankrade implantat som idag är en vanligt förekommande behandlingsmetod för att återställa förlorade kroppsfunktioner. Genom att förankra implantatet direkt i benet överförs effektivt påförda laster till skelettet vilket ställer höga krav på implantatmaterialen. Man ser en växande efterfrågan på nya material med optimerade egenskaper för tillämpningar ämnade för en snabbare och säkrare behandling. Samhällsbehovet växer allteftersom den förväntade livslängden fortsätter att öka med en växande åldrande befolkning som följd.

Syftet med avhandlingen var att öka förståelsen för hur olika faktorer påverkar stabiliteten av benförankrade implantat, speciellt med avseende på implantatets ytkemi, yttextur och belastning. Metodiken varierade från bänkförsök, datorsimuleringar, experimentella djurförsök till belastningsmätningar på amputationspatienter med benförankrade proteser.

Resultaten visade att ytkemin påverkar benbildning runt implantatet där en låg halt zirkonium (Zr) tillsatt till additivt tillverkade implantat av kobolt (Co), krom (Cr) och molybden (Mo) gav en stabilare förankring i kanin. Dessutom visades implantat tillverkade i en ny legering bestående av titan (Ti), tantal (Ta), niob (Nb) och Zr integrera likvärdigt med kommersiellt ren Ti i råtta. För att systematiskt undersöka vilken effekt ytstrukturrelaterade faktorer har på stabiliteten utvecklades en experimentell modell, där vridmomentet analyserades efter att implantaten gjutits in i härdplast. En tredimensionell datormodell av det experimentella försöket utformades där ytstrukturen varierades för att studera retention och frakturer i gränsskiktet mot implantatet. Analyserna visade att ytstrukturen såväl som det omgivande material har stor betydelse för stabiliteten. För att studera belastningens inverkan på benet utfördes belastningsmätningar på amputationspatienter med benförankrad protes då de utförde en vardagsaktivitet. Lastfördelningen kring benförankringen simulerades i en datormodell och visade på nivåer som kan orsaka benresorption i gränsskiktet mot distansen. Dessutom analyserades benvävnad uttagen från en patient vid implantatbyte för att fastställa gränsskiktets status efter långvarigt användande.

Sammanfattningsvis, implantatets ytegenskaper kan modifieras för att uppnå en stabilare biomekanisk förankring och en fördelaktigare lastöverföring och minskar därmed risken för implantatförlust och komplikationer för patienten.

LIST OF PAPERS

This thesis is based on the following studies, referred to in the text by their Roman numerals.

I. Stenlund P, Kurosu S, Koizumi Y, Suska F, Matsumoto H, Chiba A, Palmquist A. Osseointegration Enhancement by Zr doping of Co-Cr-Mo Implants Fabricated by Electron Beam Melting.
Additive Manufacturing. 2015;6:6-15.

II. Stenlund P, Omar O, Brohede U, Norgren S, Norlindh B, Johansson A, Lausmaa J, Thomsen P, Palmquist A. Bone response to a novel Ti–Ta–Nb–Zr alloy.
Acta Biomaterialia 2015, In press

III. Stenlund P, Murase K, Stålhandske C, Lausmaa J, Palmquist A. Understanding mechanisms and factors related to implant fixation; a model study of removal torque.
J Mech Behav Biomed Mater 2014;34C:83-92.

IV. Murase K,* Stenlund P,* Nakata A, Takayanagi K, Thomsen P, Lausmaa J, Palmquist A. 3D modeling of surface geometries and fracture progression at the implant interface.
In manuscript.

V. Stenlund P, Trobos M, Lausmaa J, Brånemark R, Thomsen P, Palmquist A. The effect of loading on the bone around bone-anchored amputation prostheses.
In manuscript.

* *Equal contribution*

CONTENT

1 INTRODUCTION

1.1 Background

The human skeleton is a unique living organ with a load-bearing capacity as its main function. Bone-anchored implants are nowadays a commonly used treatment to restore lost body functions by serving as anchorage points for prostheses. The direct fixation of implants in the bone enables an effective load-transfer to the surrounding skeleton. Examples of bone-anchored implant applications are oral and maxillofacial reconstructions, hearing aids, joint replacements and amputation prostheses. The most commonly used materials are different grades of titanium (Ti) depending on the load-bearing requirement. The demands imposed on the material are constantly raised stressing the development of new biomaterials with improved mechanical strength and advantageous surface properties. Devices with new complex designs intended to withstand high loads have been introduced as well as applications where reduced implant dimensions are needed. Furthermore, with an increasing life expectancy and a growing elderly population as a result we can expect the number of patients needing treatment to increase with time. This is a major challenge for the society and calls for efficient treatments with predictable, high success rates. Still, identifying the mechanisms controlling the tissue response to different surface properties and mechanical loads has proven quite difficult due to the large variety of available factors, emphasizing the need for systematic studies. A deeper understanding of how different factors influence the bone tissue and implant stability can help to optimize material and surface properties. This can in turn minimize the risk of implant failure, reduce rehabilitation time, pain and suffering for the patient with the benefit of reducing socioeconomic costs.

1.2 Bone

Bone has several functions including supporting the body, protecting organs, producing hormones and being a mineral reservoir. Bone continuously undergoes changes as a response to mechanical or hormone stimuli in order to maintain these body functions throughout life. Therefore the anatomy differs considerably in size, geometry and organization throughout the body. Bone is a composite material consisting of different types of cells and a mineralized extracellular matrix (ECM) composed of an organic and an inorganic phase. The organic phase of the ECM contains collagen fibers, mainly collagen type I, and non-collagenous proteins. The inorganic phase of the ECM is hydroxyapatite, a calcium phosphate mineral. The organic phase provides tensile strength and elastic properties while the mineral phase gives the bone strength and rigidity. The tensile strength of bone is similar to that of cast iron but with one third its density and ten times more flexible.[1]

1.2.1 Bone cells

There are several types of specialized cells populating the bone responsible for maintaining the tissue. Osteoblasts are mononucleated cells that form new bone by depositing an immature bone matrix called osteoid, and later mineralizing it.[2] Additionally, the osteoblasts mediate bone resorption by activation of osteoclasts,[3] multinucleated cells that resorb bone. The osteoclasts have also been suggested to regulate osteoblast differentiation.[4] During bone formation osteoblasts become embedded within the bone structure, in lacunae, and gradually differentiate into osteocytes. The osteocytes are interconnected and communicate with each other and the surrounding medium through their extended plasma membrane. Therefore they are believed to act as mechanosensors, instructing the osteoclasts and osteoblasts where to resorb and form bone, respectively.[5-9] At the end stage of bone formation the cuboid shaped osteoblasts will line up at the bone surface and differentiate into lining cells. These cells have a flattened morphology and expose the mineralized bone surface to osteoclasts during initiation of bone resorption.[1,10]

1.2.2 Bone structure

Bone is typically categorized as either cortical bone or cancellous bone with porosities approximately 10% or between 50–90%, respectively.[1,11] Cortical bone is compact with a highly organized lamellar structure of interconnected osteons and accounts for about 75% of the total bone volume. The osteons are composed of concentrically organized layers, lamellae, surrounding a Haversian canal containing blood vessels and nerves. These canals are further interconnected by oblique Volkmann´s canals (Figure 1). Bone lamella consists of bundles of collagen fibrils that are organized in a repetitive formation and are embedded with mineral-phase.[12] The osteocytes are interconnected by their filopodia, cytoplasmic processes, that project into small canals in between the lacunae called canaliculi.[11] The cancellous bone structure is sponge-like and can be described as an open irregular cellular network of rods, called trabeculae. The trabeculae become plate-like and more closely packed as the bone density increases.[13] The trabeculae also consist of a lamellar organization but lack the Haversian system. Most of the human bones consist of a cortical shell surrounding an inner cancellous structure occupied by bone marrow. The cancellous bone is more frequently observed closer to the joints.

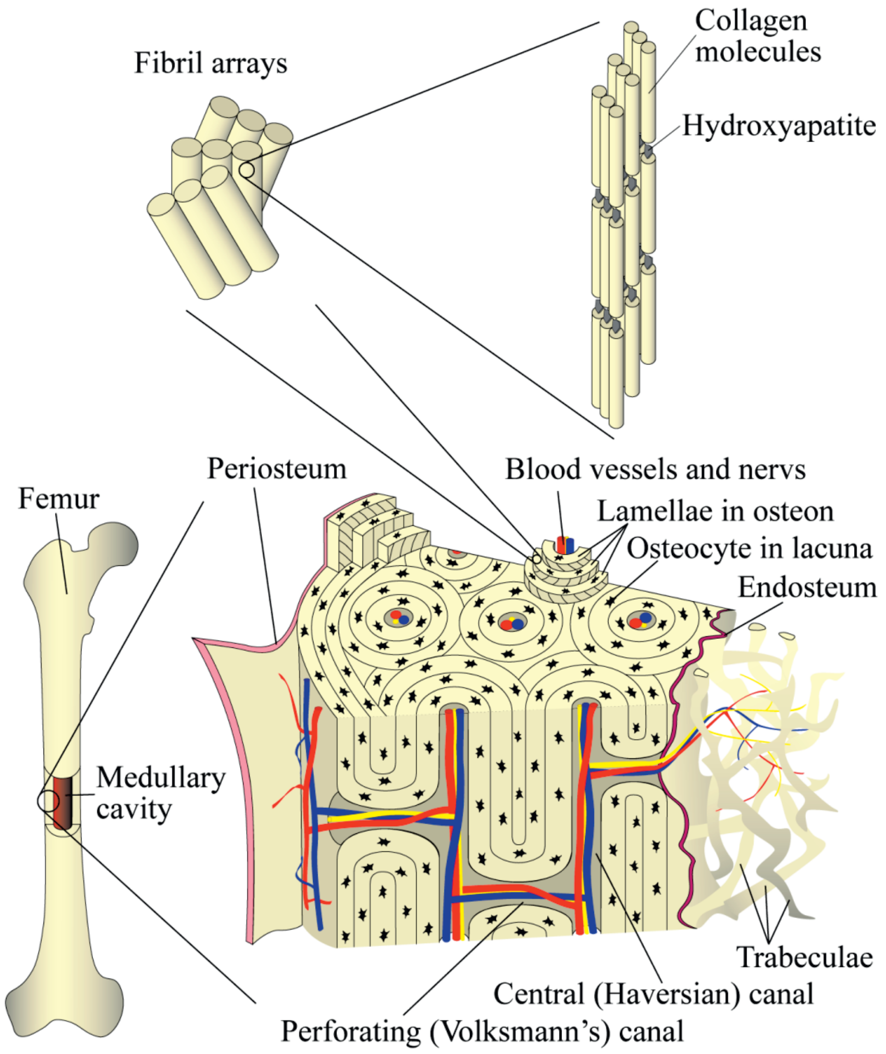

Figure 1. Schematic drawing of the bone structure from macro to nanometer level.

1.2.3 Bone modeling

Bone modeling refers to morphological or structural changes which are the result of bone formation at sites that have not undergone prior resorption. This process occurs either by endochondral or intramembranous ossification, both common during embryonic development of different types of bones and natural healing of bone fractures.[14-16] Briefly, endochondral bone formation consists of the following; a cartilage template is built by mesenchymal stem cells that differentiate into chondrocytes, after which osteoblasts subsequently replace the cartilage tissue by mineralized bone. Intramembranous bone formation begins in highly vascularized connective tissues and in hematoma during fracture healing, wherein mesenchymal stem cells cluster and start to differentiate into osteoblasts. The osteoblasts then produce osteoid and contribute to its mineralization.[17]

1.2.4 Bone remodeling

Bone remodeling refers to the coupling between bone resorption and bone formation within basic multicellular units at the bone surface. When the process is initiated, the lining cells will retract and expose the mineralized bone surface. Osteoclast precursors are recruited from the circulation, differentiate into multinucleated osteoclasts and attach to the bone surface. Osteoclasts will then start to degrade the bone matrix by lowering the local pH resulting in the release of growth factors (Figure 2 and 3).

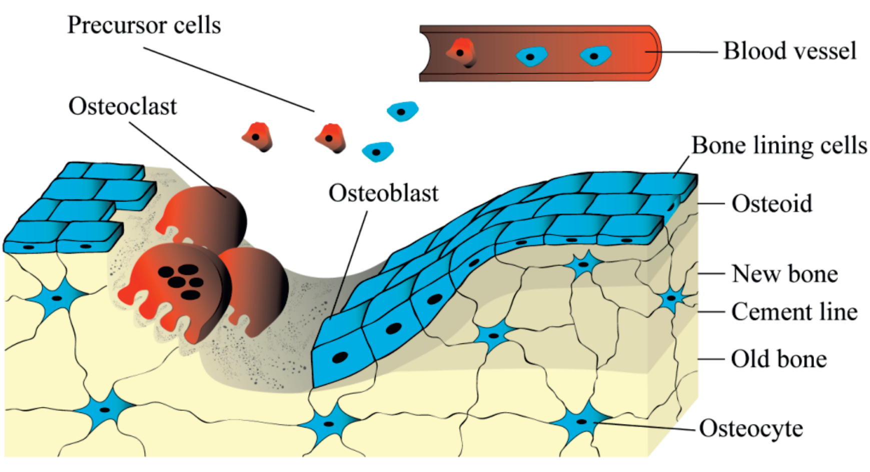

Figure 2. A schematic cross-section of bone during bone remodeling at the surface with coupled osteoclastic and osteoblastic activity. (Inspired by Seeman and Delmas,2006)[18]

These may recruit osteoblast progenitors and promote their differentiation to mature osteoblasts. The osteoblasts fill the resorption pits with newly formed osteoid, in which some osteoblasts become embedded as osteocytes while other transform into lining cells. Thereafter mineralization occurs and the remodeling is complete. The complex cross-talk between the cells within the unit is regulated by a coordinated exchange of signals. However, all the factors and mechanisms involved are yet not fully understood. This dynamic process is both constant and central to maintaining the mechanical integrity of the skeleton, which needs to adapt to variable mechanical loading, repairing damaged bone and acting as a storage facility for systemic mineral homeostasis. The metabolic rate of trabecular bone is about ten times that of cortical bone due to the higher bone surface to volume ratio of trabecular bone. This results in renewal of approximately 5–10% of the total bone per year.[4,19-22]

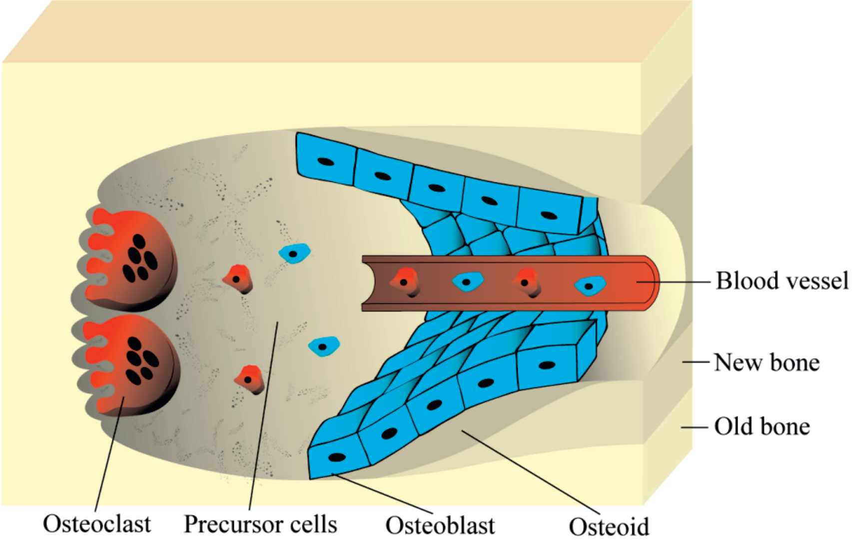

Figure 3. A schematic cross-section of bone undergoing remodeling with coupled osteoclastic and osteoblastic activity during formation of a Haversian system.

1.3 Bone mechanics

1.3.1 Basic mechanical concepts

The strength of a material is its ability to resist deformation and failure when subjected to a load. To describe this relationship quantitatively, the terms strain and stress are used in mechanics. Stress (σ) is defined as the force (F) per unit cross-sectional area (A), according to Eq. 1.

$$\sigma = F / A \qquad \text{(Eq. 1)}$$

The basic unit of force is *newton* (N) and that of length is *meter* (m) and thus the basic unit of stress is *newton per square meter* (N/m^2) or *pascal* (Pa) expressed in the International System of Units (SI units). When stress is applied *in vivo*, it can generally be seen as the interaction between materials in different parts of the body.

Strain (ε) describes the stress-related deformation of solids, and is defined as the relative length deformation (δ) per unit of the original length (L) over which the deformation occurred, and is according to Eq. 2 hence dimensionless.

$$\varepsilon = \delta / L \qquad \text{(Eq. 2)}$$

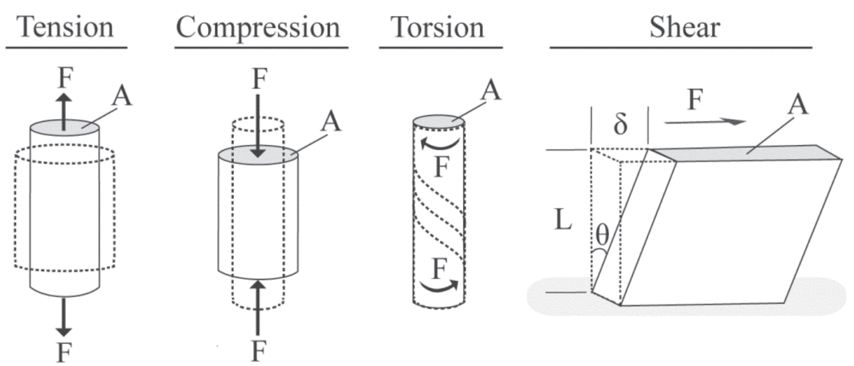

Figure 4. Schematic of specimens subjected to different type of loading. Dotted lines show the shapes prior to loading. Loads (F) are indicated by arrows, the area (A) is marked in grey. The initial length (L), deformation (δ) and angular displacement (θ) during shear loading has been indicated.

Tensile stress causes elongation while compressive stress causes compression of the material on which the stress is acting (Figure 4). Most engineering materials are Hookean elastic solids for which the stress is linearly proportional to the strain below the yield limit of the material. They obey Hooke's law, Eq. 3, where the material constant (E) is called the elastic modulus or Young's modulus, and reflects the material stiffness. Graphically it can be defined as the slope in the linear portion of the elastic region of the stress-strain plot (Figure 5).

$$\sigma = E\varepsilon \qquad \text{(Eq. 3)}$$

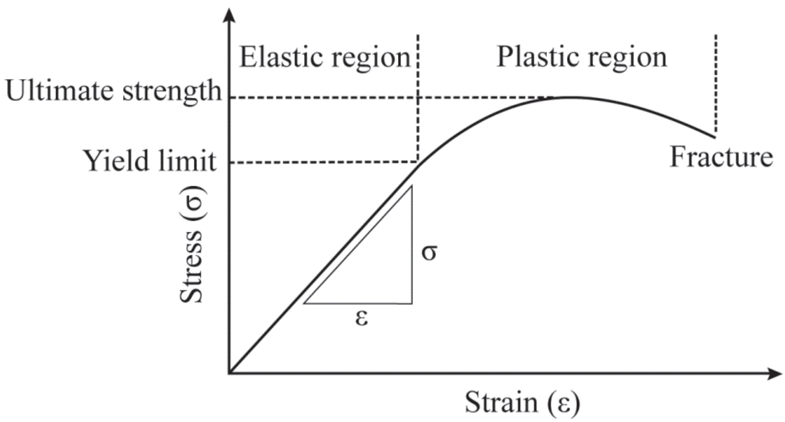

Figure 5. Schematic stress-strain plot for elasto-plastic materials.

The material will deform plastically when subjected to stresses above the yield limit and eventually fracture. When a structure is loaded in torsion, the applied load causes it to twist around its neural axis (Figure 4), resulting in shear stresses in the material. Shear stress (τ) is the result of force acting parallel to the area supporting it (Eq. 4) causing a dimensional change (δ) to occur. The shear strain (γ) is related to the angular displacement (Figure 4) and defined as the tangent of the angle (θ). For small deformations the tangent of the angle can be approximated to the angle, according to Eq. 5.

$$\tau = F / A \qquad \text{(Eq. 4)}$$

$$\gamma = \tan(\theta) = \delta / L \approx \theta \qquad \text{(Eq. 5)}$$

The basic unit of shear stress is the same as for stress, *newton per square meter* (N/m^2) or *pascal* (Pa). Shear strain is a relative quantity and hence dimensionless. The toughness of a material is defined as the work required making the material to fracture, the area under the load-deformation plot, which reflects the energy absorption ability of the material. There are materials with more complex mechanical behavior such as decreasing stress magnitudes when subjected to constant strain, known as stress relaxation. Some materials continue to deform, they are said to creep, when subjected to a constant stress level. Hysteresis describes the phenomenon seen during cyclic loading for which the stress-strain relationship differs during the loading and unloading process. Phenomena which are features of viscoelasticity include stress relaxation, creep and hysteresis.

1.3.2 Mechanical properties of bone

Bone is a complex, highly organized tissue with a non-homogeneous anisotropic composite structure[23]. It consists primarily of collagen and mineral, for which the amount, arrangement and molecular structure determines the mechanical properties of the bone.[24,25] Consequently, the properties vary with the orientation, size and shape of the ultimate bone structure.[26,27] With time, bone adapts to the load situation by optimizing the size and geometry to achieve more advantageous stress and strain levels in the bone.[24,28,29] Several mechanical quantities have been found to influence the bone modeling and remodeling e.g., the load magnitude, frequency and strain rate.[30-35] Most bones are stronger in compression than in tension and even weaker in shear.[36] The laminar structure of cortical bone gives it much higher strength and modulus of elasticity than that of cancellous bone.[37] The mechanical properties of bone have also been shown to vary with the anatomical site[26,38], age[39-41], density[38] and depend on the mechanical test, sample condition and geometry.[42] The cortical bone typically has a density of approximately 1.8 g/cm^3 whereas the density of cancellous bone varies in the range 0.1–1.0 g/cm^3. The strength and modulus of cancellous bone have been shown to vary approximately with the square of the apparent density,[31,43] typically corresponding to values in the range 0–17 MPa and 0.1–1 GPa, respectively.[38,44] The elastic modulus of the femur diaphyseal cortical shell has been reported to approximately 11.5 and 17 GPa in the transverse and longitudinal direction, respectively.[26,27,45,46] Moreover, the bone has been shown to be viscoelastic i.e., time dependent,[47] where the response is dependent on the rate at which the loads are applied. When loaded at high rates the bone can withstand greater loads before it fractures compared to when it is subjected to slowly applied loads. Several physical processes have been proposed to contribute to the viscoelasticity of bone e.g., the motion of fluids in bone canals, inhomogeneous deformation of osteons, lamellae, cement lines, fibers and molecular modes in collagen.[48] Bone behaves similar to Hookean elastic solids under certain conditions namely, low loading rates and below specific stress and strain limits. Materials are generally affected by fatigue, which reflects the interplay between the load and the number of repetitions. Fracture may occur for a few high loads or for relatively low loads repeated several times.[49] Bone fractures results from crack propagation following extensive microdamage to the bone matrix.[50-53] However, the remodeling process of living bone constantly repairs microdamage in the matrix[11,54] but fatigue fractures will result if the damage out-paces the remodeling process.[55,56] More information about the general biomechanical aspects of bone can be found in other sources.[24,57-59]

1.4 Biomaterials in bone

A biomaterial is a material used in a device, intended to interact with a biological system.[60] These materials need to be safe, biocompatible and meet the requirements of their specific applications to be successful *in vivo* and in the clinic. When introduced in bone tissue some materials have the ability to be integrated, a phenomenon referred to as osseointegration.[61] It has been defined as the direct anchorage of an implant by the formation of bony tissue around the implant without the growth of fibrous tissue at the bone-implant interface.[62] Metallic biomaterials are commonly used in medical devices to replace or restore lost body parts and functions, primarily in the fields of orthopedic surgery and oral and maxillofacial surgery.[63] Metallic materials are favorable in these applications due to their high strength, toughness and durability. Corrosion- and wear resistance of the materials used *in vivo* are important requirements since metal ion dissolution or wear debris might induce toxicity.[64,65] In the specified fields pure Ti, Ti based alloys such as Ti–6Al–4V made of Ti, aluminum (Al) and vanadium (V), Co–Cr–Mo alloys made of cobalt (Co), chromium (Cr) and molybdenum (Mo), and high grade 316 stainless steel are currently the most commonly used materials.[66]

1.4.1 Material properties

Titanium has several material properties that are advantageous for medical devices e.g., a high strength/weight ratio, biocompatibility, inert character and excellent corrosion resistance. Additionally, Ti has an elastic modulus that is approximately half that of Co–Cr and stainless steel. Consequently, it is less likely to cause stress shielding in bone applications.[67,68] The introduction of alloying elements such as Al, V, niobium (Nb), tantalum (Ta), Mo and zirconium (Zr) to Ti, changes the material properties. Depending on the resulting microstructure, the Ti alloys are categorized as either α, β or α–β type.[69-71] The Ti–6Al–4V is a commonly used alloy of α–β type with enhanced strength and workability compared to pure Ti, and it is commonly used in the medical field. Modified Ti alloys are constantly finding new applications in medical devices.[69] One characteristic of Ti is that it is a very reactive material that spontaneously forms a stable oxide film (TiO_2) when in contact with water molecules or air. Different surface modifications and oxidation treatments can be used to further enhance the biological, chemical and mechanical properties of the material.[72] Stainless steel is an iron (Fe) based alloy (<50 wt% Fe) with at least 12–13 wt% Cr addition. By incorporating other elements such as nickel (Ni) and Mo to the composition the corrosion resistance is improved while the strength is decreased. The latter can, however be counteracted by working, heat treatment and hardening. In contrast to Ti based materials, stainless steels possess excellent torsion and elongation properties that are well suited for sternal and bone fixation wires applications.[66] Co–Cr alloys have excellent wear resistance which makes the material well suited for sliding parts in joint implants, in for example the knee and hip.[67,73] The metal is typically cast, due to its low plasticity which makes it difficult to work. However, heat treatment and cold working can improve the strength and elongation attributes of Co–Cr alloys to similar levels or higher than those of stainless steels used in applications such as orthodontic arch wires, clips and catheters.[66,74]

1.4.2 Bone healing and remodeling around implants

Bone regeneration around implants resembles the intramembranous bone formation with succeeding phases of inflammation, regeneration and remodeling. The initial response when a foreign material is introduced in the body involves the following: protein adsorption, platelet activation, coagulation and inflammation. The surgical trauma following the implant insertion causes damage and thermal necrosis of the bone. A blood clot is formed at the bone-implant interface promoting the establishment of a well-vascularized, immature connective tissue followed by osteogenesis. The bone forms either on the implant surface by contact osteogenesis or it forms from the existing bone towards the implants surface by distance osteogenesis. The implant can act as an osteoconductive substrate and its surface has been shown to influence the biological components and thus the healing events. More details can be found in the referred reviews.[75-77] Additionally, mechanical loading can stimulate the healing process as previously described in the paragraph "mechanical properties of bone". However, excessive micromotions at an implant interface will disturb the osseointegration process and result in formation of a fibrous tissue capsule around the implant and may eventually lead to implant failure.[78,79]

1.4.3 Selected biomaterial interfaces

Since Professor Per-Ingvar Brånemark introduced Ti in the 1960's it has found ever-increasing application in medical devices in the oral,[61] maxillofacial[80,81] and orthopedic field.[82] Implants generally initiate a transient inflammatory response when introduced in the tissue followed by a fibrous encapsulation in soft tissue and osseointegration in bone.[83] Dental implants, hearing aids and amputation prostheses are all examples of percutaneous bone-anchored applications where the implant system penetrates the mucosa or the skin, the body's external barriers. These interfaces are unique since they are in contact with both bone and soft tissues and facing the challenge to maintain the barrier while restoring the lost body function. Based on natural penetrations like teeth, the percutaneous implant is more likely to be successful if the implant-soft tissue interface is tight, in good health and minimize relative motions. However, a detailed understanding of how different material/implant surface properties affect the tissue response is yet lacking. Despite high success rates, skin or mucosa penetrating implants are associated with certain failure modes[84]:

- *Marsupialization*: encapsulation by epidermal downgrowth along the implant interface, generally not occurring around Ti implants

- *Permigration*: formation of an immature connective tissue not able to nourish the downward migrating epidermis into the structure of porous implants

- *Avulsion*: mechanical disruption of the skin surrounding the implant followed by microhematoma and subsequent inflammation

- *Infection*: invasion and multiplication of microorganisms, typically bacteria, triggering an adverse host tissue reaction.

Oral implants

Oral implants serve as anchorage points to replace missing teeth aiming to restore the masticatory and phonetic function as well as esthetics. Stable fixations and success rates up to 99% have been reported at 20 years follow-up.[85-87] Implants retrieved after up to 16 years showed 56–85% bone-implant contact and 79–95% bone area around the implant.[88] Challenging clinical situations such as compromised bone conditions are associated with higher failure rates.[89] However, by using planning and carefully performed surgery the most severe complications can be avoided.[90] The main difference between natural dentition and oral implants is the lack of a periodontal ligament in the latter. In contrast, the soft tissue surrounding the oral implant consists of mucosa covered by epithelium and connective tissue nearer the bone crest.[14,91] An implant-tissue attachment is preferred since it resembles the natural dentition and the soft tissue serves as a defense barrier against bacterial colonization. It has been hypothesized that rougher surfaces might be advantageous for tissue-implant ingrowth. However, certain surface roughness has been reported to be more susceptible to bacterial colonization.[92] The biomechanics associated with oral implants is another important determinant for clinical success;[93] the loads induced during mastication vary in orientation, magnitude, rate and distribution pattern which in turn depends on the dental prosthesis, implant design, surface properties and the bone interface.[94] The mechanical condition might influence the observed marginal bone loss around the implant.[95] Finite element studies around oral implants have shown that the implant design, surface properties, bone and interface condition influence the load distributions around oral implants.[96-98] The most widely used commercial dental implants show a variety of surface properties which need to be thoroughly characterized in order to elucidate their role for clinical success.[77,99-102]

Amputation prostheses

Bone-anchored amputation prostheses have proven very successful[82,103] as an alternative treatment to the conventional socket prostheses since its introduction in the early nineties.[104] In comparison to the socket-type treatment a direct fixation in the bone offers increased quality of life.[105] Some advantages are reduced pain, soft tissue irritation, improved prosthetic usage, range of motion, sitting comfort[106,107] and enhanced osseoperception: the ability to perceive the environment through the prosthesis.[108] The implant system comprises an abutment connecting the prosthesis to the bone-anchored fixture. During surgery the soft tissue is sutured to the bone around the abutment. In a comparative study, the orthopedic implants were shown to induce less intense inflammatory reaction compared with craniofacial implants.[109] The inflammatory cells were mainly located in the nearest vicinity of the implant interface and in the epidermis. Despite the presence of colonizing bacteria, the occurrence of infections that lead to disability or implant removal were few in number.[110] The follow-ups have revealed a stable fixation several years after implantation even though some observations of bone resorption around the implant have been reported.[111,112] The amputation and treatment results in altered loading conditions of the bone. Different techniques are available for measuring the weight bearing of implants, all with their own advantages and limitations.[113] Techniques that utilize a load cell directly-fixed to the implant system have proven very useful as tools for unrestricted measurement of the loads imposed on lower limb prostheses.[114-116] The loads show good agreement with the physiological loads applied to the femur during activities of daily living.[117] However, to understand how these loads affect the bone tissue the load distribution and its effect on the tissue needs to be determined. Finite element analysis is well suited to estimate the mechanical condition around complex geometries and have been applied in a limited number of studies of trans-femoral amputation prostheses.[112,118-123]

1.5 Implant stability

Implant stability can be defined as the immobility of an implant. Primary stability relates to the state immediately after placement of the implant, while secondary stability relates to the state achieved after healing has occurred.

1.5.1 Evaluation methods

There exist several methods, both invasive and noninvasive, to evaluate implant stability. Clinically, the primary stability can be assessed either by the implants cutting resistance or the insertion torque during implant placement. Additionally, different noninvasive analysis techniques exist e.g., subjective evaluation of the sound from percussion of an implant, analysis of the contact time during tapping of the implant and analysis of the resonance frequency[124] of a probe connected to the implant. Examples of invasive techniques are the following: removal torque (RTQ), pull-out and push-out tests mainly used in experimental work to evaluate the implant stability.[125,126]

Removal torque analysis

The technique is used to determine the stability of an implant by measuring the torque required to break the bone interlocking at the implant surface. The technique typically involves fixation of the test sample so that the implant axis aligns with the torque actuator in order to ensure the application of pure axial torsion. The test specimen should be kept hydrated during the whole testing procedure, minimizing risks of altering the bone properties. Testing is then performed by rotating the implant counterclockwise at a rate of typically 0.1 degree per second while continuously collecting the torque and angle data. Analysis of the torque versus angle plot gives the interfacial stiffness and the maximum removal torque value, for which the latter can be used as a measure of implant stability. The technique is applicable in experimental studies and has proven suitable in several different species.[127,128]

Additional examples on stability evaluation by removal torque analysis are described in the following paragraphs.

The finite element method (FEM)

Finite element modeling is based on simulations in a computer. The method is a powerful numerical tool that enables analysis and simulation of engineering concepts such as load distributions and displacements at the implant interface. By dividing models with complex geometries in smaller volume elements the intricate mechanical interactions can be resolved by analyzing each element separately. The properties (stiffness) of all elements and the boundary constraints between them need to be defined. During the analysis, loads or prescribed displacements are typically applied for which the displacements of individual nodes, connecting the elements together, are calculated so that equilibrium is fulfilled. Strain, stress and force distributions can then be derived. More information about the applicability of the technique in dental and orthopedic research for modeling of load distribution, bone tissue fractures and healing can be found in the referred reviews.[129-132]

1.5.2 Factors affecting implant stability

The implant and interface related factors will determine the mechanical condition and affect the biological response when introduced into the bone. These are therefore vital for the implant stability, which is a prerequisite for clinical success.

Implant design

Implants are designed to facilitate placement and achieve a strong fixation that distributes the load appropriately. By using theoretical and numerical analysis the implant design has been shown to affect the interfacial shear stress levels and distribution in the bone surrounding the implant. The studies revealed that excessive magnitudes might cause bone loss and hence reduce the implant stability.[133-137] Finite element analysis has been used to show that a more homogenous load distribution can be achieved by changing the thread design[138] or reducing the implant stiffness.[139,140] Additionally, implant modifications such as increased diameter, tapered shape, or changed thread design have been shown to improve the mechanical fixation experimentally.[141-144] Bone ingrowth into porous designs increase the implant stability and have been shown to be pore size dependent.[145,146]

Surgical protocol and precision

The surgical technique was found to affect the primary stability when the implant site was prepared by either press-fit or undersized technique.[147-149] FEA shows that the applied torque values strongly influence the stress patterns in the bone.[150] Higher insertion torques have been shown to increase the primary stability of implants without causing necrosis of the bone or implant failure.[151,152]

Bone status and interface condition

Contact between the implant and bone is a prerequisite to prevent movement at the interface and hence achieve a stable integration. Bone density has been thoroughly evaluated and correlates with the primary implant stability.[153,154] The secondary stability measured by removal torque was found to correlate with the bone-implant contact *in vivo* using a rat tibia model with a healing period of 16 weeks.[127] Additionally, in studies using FEA the stress and strain distribution around dental implants were influenced by the osseointegration level,[155] contact situation and bone properties.[96,98].

Surface topography

Over the years various approaches to improve and interpret the biological response to surface modifications have evolved. The role of surface roughness[156] on interfacial shear strength has been defined mathematically using theoretical models in order to optimize the mechanical response.[157-160] The importance of surface topography for mechanical retention has also been evaluated experimentally.[161] Increased surface roughness correlates with the bone-implant contact[162,163] indicating contact osteogenesis, and resulted in stiffer bone[164] and higher removal torque values after healing *in vivo* both in rat,[165] rabbit[166-172] and canine.[173,174] Implants and scaffolds produced by additive manufacturing[175] having a native surface topography at least ten times the scale of conventional dental implants have shown promising both *in vitro*[176,177] and *in vivo.*[178-180] Moreover, porous coated hip-replacements have been evaluated clinically with positive outcomes.[181,182] For the interested reader there are several reviews on the topic of the effects of surface topography on the bone response.[183-186]

Surface chemistry

The elemental surface composition is important for the material biocompatibility[187,188] and has been shown to affect the bone response in numerous occasions for implants placed in different species *in vivo*. For example, Ti–6Al–4V was found inferior to cp-Ti in rabbit with regard to implant fixation *in vivo*[189] while comparable stability was found for Ti–Ta–Nb–Zr in rat.[190] Different *in vivo* studies evaluating specific chemical compositions in comparison to cp-Ti showed that addition of Zr or Mg to Ti implants resulted in stronger bone fixation in rabbit,[191-193] Zr[194] or Ti–6Al–4V[195] implants both showed less collagen content in the bone in the nearest vicinity of the implant, and faster mineralization of bone was noticed around the Zr implants.[196] Co–Cr–Mo implants have been observed to osseointegrate to a degree similar to that of Ti in several studies but indications of decreased stability around the Co–Cr–Mo implants have been reported.[197,198] However, the addition of Zr to the Co–Cr–Mo composition enhanced the implant fixation.[180] Cellular and molecular surface modification approaches have also been suggested as strategies to direct the biological response at the interface.[199,200]

Mechanical loading

Implant loading directly affects the remodeling process around implants and hence bone-implant interfacial conditions. All the previously discussed factors affect the bone-implant interface, which in turn alters the load distribution around the implant. The mechanical stimuli will then affect the bone response and with time change the stability of the implant. The effect of loading has been evaluated in different species *in vivo* and was found to influence the bone modeling and remodeling around implant in rat,[30] rabbit,[201] guinea-pigs,[35] canine[202] and monkey.[203] The effect of loading on skeletal adaptation has been thoroughly reviewed by different authors.[21,204-207]

2 AIMS

The aim of this thesis was to gain a deeper understanding of the factors contributing to the fixation of bone-anchored implants, especially with regard to surface topography, surface chemistry and implant loading. The methods used in the thesis to address the aims range from systematic bench studies, computer simulations, experimental *in vivo* studies, to load cell measurements on patients treated with bone-anchored amputation prostheses.

The specific aims of the five studies included in the thesis were the following:

- Evaluate the influence of surface chemistry on the bone anchorage and osseointegration performance by studying EBM-produced implants of Co–Cr–Mo alloy and the effect of an addition of 0.04 wt% Zr to the starting powder metal in a rabbit model after 8 weeks *in vivo* (Paper I) and a novel Ti–Ta–Nb–Zr alloy in a rat model for 7 and 28 days *in vivo* (Paper II).

- Develop a bench model to study removal torque and implant stability related factors. A secondary aim was to identify factors contributing to anchorage of an implant (Paper III).

- Propose a finite element model for the fracture progression at an implant interface by simulating the micron scale interface of a macro removal torque model. A secondary aim was to evaluate the influence of the shape of surface elements on the retention (Paper IV).

- Investigate the stress and strain distributions involved during loading of trans-femoral osseointegrated implants. A secondary aim was to evaluate the tissue at the transcutaneous region for a patient undergoing implant revision (Paper V).

3 MATERIALS AND METHODS

3.1 Implants

The materials and implants/samples used in the different studies were the following:

- Experimental Co–Cr–Mo alloy solid implants, total length of 4 mm and Ø 3.75 mm, manufactured by EBM in an Arcam EBM A2X system by Institute for Materials Research, Tohoku University, Sendai, Japan (Paper I).

- Experimental Ti grade IV and Ti–Ta–Nb–Zr alloy mini-implants, total length of 2.3 mm and Ø 2 mm, manufactured by Cendres+Métaux SA, Switzerland (Paper II).

- Experimental Ti grade IV implants and cylinders, Ø 3.75 and 3 mm respectively, total length of 10 mm (implant threaded part 6 mm), manufactured by Elos Medtech Pinol A/S, Denmark (Paper III).

- Commercial OPRA (Osseointegrated Prostheses for the Rehabilitation of Amputees) implant system, threaded fixture with a total length of 80 mm and Ø 16 mm, abutment with a total length of 72 mm and Ø 11 mm, Integrum AB, Sweden (Paper V).

3.1.1 Electron beam melting

The implants in Paper I were made from gas atomized spherical Co–Cr–Mo powders, with and without the addition of 0.04 wt% Zr (Sanyo, Hyogo, Japan). The size distribution of the powder particles were between 25 and 150 µm, with average diameters of 100.7 and 102.3 µm for Co–Cr–Mo and Co–Cr–Mo–Zr, respectively. The chemical composition of the powders was in accordance with ASTM F75 standard. The same parameters were used in the EBM process for both materials; 750–850 °C build table temperature, vacuum of ~10^{-3} mbar, layer thickness of 70 µm and subsequent cooling in helium. The implant was built layer by layer from a 3D computer-aided design (CAD) model by selective melting of metal powder using an electron beam in a high vacuum. The procedure briefly consists of the following: one layer of metal powder is laid out and preheated on the starting plate, followed by selective melting of the powder to create a cross-section of the build, then the stage is lowered by the height of one build layer, after which the process is repeated until the entire build has been finished. The material, method and post-processing should be aimed to meet the requirements of the intended application.

3.2 Surface treatments

The typical implant manufacturing techniques result in rather crude implant surfaces that normally also become contaminated during the process. The desired surface properties can be achieved in numerous ways.

3.2.1 Chemical

Acid etching (pickling) was used to modify the surface topography in order to achieve uniform roughened surfaces by removal of the oxide scales and plastically deformed surface layers. The etchants used were HF/HNO_3 (Paper III), HF/HNO_3 and HCl/H_2SO_4 (Paper II). To reduce surface contaminations the materials were ultra-sonically cleaned for a few minutes using either a series of different solvents (heptane, acetone and ethanol) or a tenside-based cleaning solution (MIS 024, Tremedic AB, Sweden). Sterilization by autoclaving was performed on all implants prior to implantation *in vivo* (Paper I and II).

3.2.2 Electrochemical

Electropolishing is a technique where the surface layer is modified by electrochemical dissolution to produce a smooth finish. In Paper III, electropolishing was performed in an electrolyte consisting of perchloric acid, methanol and n-butanol at a temperature of –26°C and 22,5 V anodic potential for 3 minutes.[208]

3.3 Characterization techniques

Characterization techniques are used to analyze, monitor or verify certain aspects of the material surface. In order to gain an as detailed description of both qualitative and quantitative properties as possible it is necessary to use different techniques.

3.3.1 Chemical composition

The X-ray photoelectron spectroscopy (XPS) technique was used to quantify the relative elemental chemical composition of the outermost 2–10 nm of the material surface (Paper I and II) as well as measuring a depth profile of selected elements (Paper I). In Paper I, survey (Ø 2 mm) and regional (Ø 110 µm), high energy resolution scans of the surface as well as a depth profile were acquired by alternating spectrum acquisition and sputtering off layers using an inert argon gas ion gun (Kratos Axis ultra DLD). In Paper II survey and regional scans were acquired from the top of two threads (Physical Electronics, Model PHI 5500).

In Paper II inductively coupled plasma–optical emission spectroscopy (ICP–OES) was used to quantify the absolute chemical composition of Ti, Ta, Nb, Zr and trace elements averaged over the entire sample (Spectro-Arcos). Lighter elements, C, O, N and H, were identified with different LECO instruments TC–436 (Paper I), TCH600 and SC600 (Paper II) using He as an inert gas and a temperature of about 2200 °C.

Hydrophobic and hydrophilic properties were evaluated by water contact angle measurement (Fibro-DAT1100, Fibro System AB). The contact angle was determined for 4 µl droplets of deionized water applied to 4 etched disks of each material after a stabilization time of 10 s (Paper II).

3.3.2 Surface topography

Qualitative evaluation of the surface morphology was performed by scanning electron microscopy (SEM) in the range 50× to 200,000× magnification using an acceleration voltage between 1–5 kV in secondary electron mode by a Leo Ultra 55 (Leo Electron Microscopy Ltd., UK) in Paper I and a Supra 40VP (Zeiss, Germany) in Paper I, II and III.

Quantitative evaluation of the surface topography was achieved by the different analysis techniques. Confocal laser microscopy (HD100, Lasertec, Japan) was used in Paper I, with a scanning area of 0.33×0.33 mm. 3D-SEM (Supra 40VP, Zeiss, Germany) was performed in the range 200× to 10,000× magnification using an acceleration voltage of 5 kV in secondary electron mode and 8° or 20° eucentric tilt reconstructed and analyzed using MeX 6.0 ed. Alicona, Austria (Paper I, II and III). Optical profilometry (Veeco NPFlex 3D, Bruker, USA) was performed at 27.4× magnification in the VSI mode on a surface area measuring 0.174×0.232 mm, cylinders were corrected for form and tilt while screw shaped implants were corrected by a high-pass Gaussian filter with a cut off frequency of 45 µm (Paper III). The analyzed surface roughness parameters were; S_a (arithmetical mean height), S_{sk} (skewness of height distribution), S_{ku} (kurtosis of height distribution), S_{dq} (root mean square gradient), S_{dr} (developed surface area ratio) and S_{ci} (surface core fluid retention index).

3.4 In vitro cytotoxicity

In vitro cytotoxicity tests were performed in Paper II in order to study the responses to the material and identify potentially negative responses prior to implantation. The tests were in accordance with ISO 10993–5:2009 "Biological evaluation of medical devices – Part 5: Tests for *in vitro* cytotoxicity"[209,210] and were performed on disks using material extracts, n = 4 for all materials. Liquid extracts of Ti, Ti–Al–V, Ti–Ta–Nb–Zr and Cu (positive control) disks were prepared by 48 h shaking (100 RPM) in complete cell culture media (MEM including 10% horse serum, ATCC, USA) at 37 °C in tissue culture polystyrene plates, n = 4 for all materials. Polystyrene was selected as a negative control. The culture media extract volume was 1 ml per 3 cm^2 material area. Series of diluted extracts from each material were added in triplicate to subconfluent cells (L929 mouse fibroblasts) (ATCC, USA) seeded on tissue culture polystyrene and followed for 24 h. The evaluation included quantification of the total cell number, assessment of the cellular damage by quantification of the lactate dehydrogenase (LDH) activity, and a WST-1 cell proliferation assay during the last 2 h to assess the viability and proliferation of cells.

3.5 In vivo evaluation

Animal models are used to get an initial assessment of the tissue response to medical devices such as implants prior to evaluation of their performance in the human body. Additionally, animal models are suitable for studying specific mechanisms. The animal experiments were approved by the University of Gothenburg Local Ethics Committee for Laboratory Animals (Paper I: Dnr. 01/09, Paper II: Dnr. 279/2011).

In Paper I, a rabbit model with an evaluation time point of 8 weeks was used. A total of 8 female New Zealand White rabbits weighing 4–5 kg were included in the study. In brief, the surgery consisted of the following: after one week of acclimatization the animals were anesthetized and the bone bed was carefully exposed and holes were prepared. Each animal received a total of six implants; two in each tibia and one in each femur according to a predetermined schedule. The surgery was performed under aseptic conditions and the animals were given analgesics for 3 days postoperatively. They were fed a standard diet and tap water during the observation time. Eight weeks postoperatively, the animals were anesthetized and the implants were exposed enabling biomechanical assessment of the implant stability by removal torque analysis. All implants were thereafter retrieved *en bloc* with the surrounding tissue. The sample preparation for histological evaluation in brief; fixation in formalin, dehydration in ethanol, infiltrated and embedded in plastic resin, cutting and grinding to a thin (15–20 µm) central ground-section before staining. The bone-implant interface was evaluated by qualitative histology and quantitative histomorphometry measuring the bone area around the implant and the bone-implant contact using light microscopy (Eclipse E 600, Nikon, Japan) and image analysis (NIS Elements 4.12, Nikon, Japan). The bone-implant ultrastructure was evaluated for polished samples *en bloc* by backscatter SEM (Supra 40 VP, Zeiss, Germany) operated at 20 kV.

In Paper II, a rat model with evaluation time points of 7 and 28 days were used. A total of 19 male Sprague-Dawley rats, with an average weight of 350 g were included in the study. The surgery consisted of the following: the animals had general inhalation anesthesia and while the tibial metaphysis was exposed each animal received a total of 4 implants; two in each tibia, with the Ti and Ti–Ta–Nb–Zr material separated in contralateral legs. The animals were allowed free post-operative movement with food and water *ad libitum* during the observation time. At 7 and 28 days respectively, the animals were sacrificed and the implants were exposed and the stability was measured by removal torque analysis. For histology, the implants were removed *en bloc* with surrounding tissue. For reverse transcription quantitative polymerase chain reaction (RT-qPCR) analysis, the retrieval was achieved by unscrewing the implants and retrieving the peri-implant bone by trephining. The RT-qPCR analysis was performed for the samples from 3 animals at the 28 day time point. The RNA expression was quantified for the following genes: tumor necrosis factor–α (TNF–α), interleukin–1β (IL–1β), runt-related transcription factor–2 (Runx2), osteocalcin (OC), tartrate-resistant acid phosphatase (TRAP) and cathepsin K (CatK) to determine the following ongoing cellular processes; inflammation, bone formation and remodeling either at the interface or in the peri-implant bone, respectively. In the approach where the implant was retrieved *en bloc* the bone-implant interface was also evaluated by histological and ultrastructural analysis according to the protocol described above.

In Paper V, a tissue sample from an amputation patient undergoing implant revision was retrieved and analyzed by X-ray microtomography (Skyscan 1172, Bruker microCT, Belgium). The equipment was operated at 72 kV and micrograph acquisition was performed using a pixel size of 26.4 µm and a step size of 0.7 degree/s through 180° rotation. The reconstruction and analysis was performed with regard to bone volume, trabecular thickness and separation as well as the mean distance between the bone-abutment interface using Skyscan software package (NRecon 1.6.8.4, CTvox 2.5.0 r892, CTan 1.13.4.0 and CTvol 2.2.3.0). The sample was thereafter processed for histology according to the protocol described above and quantitative analyses were performed with regard to the amount of mineralized tissue, soft tissue thickness, and epithelial down-growth. Qualitative analysis was done by characterizing the different tissues and cells, bone remodeling, vascularization, bleeding and signs of inflammation. Ethical approval was received from the local Swedish Ethical Committee (EPN/Gothenburg Dnr. 434–09).

3.5.1 Removal torque evaluation

Implant stability was evaluated by removal torque analysis. In brief, the procedure consists of the following: the sample is fixed and the implant is connected to a torque gauge by a special connector ensuring a linear alignment and pure axial torque. Thereafter, the torque response is monitored in real-time, recorded at a frequency of 4 Hz, while rotating the implants at a constant angular speed. The RTQ apparatus is a custom made upgrade of a previously described equipment.[211] In Paper I and II the rotation speed was set to 0.2 degree/s while different speeds, 0.1, 0.3 and 0.6 were used in Paper III. All load deformation plots were evaluated with regard to the maximum torque value and shape of the curve, which typically involves an initial stabilization phase followed by a linear increase in torque. During the course of the measurement, surrounding material will start to deform plastically and then fracture causing a drop in the torque that finally levels out in an interfacial friction phase.

3.5.2 Load-cell analyses

Site-specific loading analyses were performed on patients with unilateral transfemoral amputation treated with osseointegrated implants in order to determine the loads applied on the implant system (Paper V). The load cell (iPecs™ Lab, College Park Industries, USA) was fitted between the abutment and the amputation prosthesis and the load measurements were carried out in a clinical environment (Lundberg Laboratory for Orthopaedic Research, Sahlgrenska University Hospital, Sweden). Normal gait was selected as an activity of daily life for which the patients were asked to walk at self-selected speed and the forces and moments in three dimensions were recorded at 240 Hz. Ethical approval was granted by the local Swedish Ethical Committee (EPN/Gothenburg, Dnr. 130–09).

3.6 Experimental bench model

Surface topography related factors were studied by embedding experimental cylinders with modified surface topography in thermosetting polymer resins with different mechanical properties (Paper III). The turned surface topography of the machined cylinders was modified by either electropolishing or acid etching according to the previously described protocols. Prior to embedding, an anti-adhesive layer was applied by spin coating. The interlocking strength was then evaluated by removal torque analysis using rotation speeds of 0.1, 0.3 and 0.6 degree/s.

3.6.1 Experimental design

A statistical experimental design was used in Paper III as a method to identify the effect of independent variables (factors) on the response as well as potential interplay between the factors within a chosen range, a low and a high level, for each variable (Paper III). A full factorial design of 3^3 with 2 replicas and a full factorial mixed model with 5 replicas were used for the Sawbones and Altropol polymers, respectively. Randomization was implemented in the designs and analyses (MODDE 7.0.0.1, Umetrics AB, Sweden).

3.7 Finite element method

The finite element method (FEM) was used to simulate the load distributions at the implant interface (Paper IV and V). In Paper IV a combined macroscopic and microscopic 3-dimensional model was developed to estimate the stress and strain distribution and fracture progression at the implant interface. The macroscopic model represented the embedded Ti cylinder used in the experimental study while a microscopic conical feature was used to model the acid etched Ti surface topography with corresponding surface roughness values. Different contact situations were simulated by introducing a gap at the interface between the surface feature and the surrounding material. The models were meshed using hexahedral shaped 1st order elements (~10,000–60,000) aiming for uniform sizing of elements irrespective of the design. The materials were assumed homogenous and isotropic, and modeled as linear elastic solids with frictionless contact at the interfaces. During analysis the Ti surface feature was displaced parallel with the interface and the reaction force in the displacement direction was calculated. The macro- and micro models were then combined by layer-wise summation of the sum reaction forces determined by the microscopic simulations with the shift-delay equal to the difference in layer displacement of the macroscopic simulations. All contact deformation analyses were performed using the software package LS-DYNA V.970 (Livermore Software Technology Corporation, USA). Thereafter, the sum reaction force was converted to removal torque.

In Paper V, a 3-dimensional symmetrical macroscopic model was built (ANSA 14.1.0, BETA CAE Systems S.A., Greece) based on the design of the OPRA implant system. The models were automatically meshed using hexahedron (~46,000) and pentahedron (~2,400) 2nd order elements with refinements in the bone-implant interfacial regions. The model interfaces were modeled either as bounded, frictionless or with some assumed friction. Friction coefficients were assumed to be 0.2 between the transplanted bone and the abutment and 0.35 between the abutment and the implant. The fixture, abutment and femur were assumed to be linearly elastic homogeneous solids. The cortical bone region was assumed transversely isotropic with elastic modulus of 16.7 GPa and 11.5 GPa, in the longitudinal and transversal direction, respectively. The transplanted bone region was assumed isotropic with elastic modulus of 0.4, 0.8 or 4 GPa. The thickness of the cortical and transplanted bone regions were 7 mm in total; 5.54+3.46 mm or 5.27+1.73 mm in the different models. A Poisson's ratio of 0.3 and 0.35 was assumed for the bone and the Ti, respectively. The site-specific tri-axial forces and moments measured with the load transducer were used to identify the extreme loads exerted on the bone-implant interface during straight walking. These extreme loads were used for the finite element analysis (ANSYS 15.0, ANSYS Inc., USA).

3.8 Statistics

Statistical analyses are fundamental tools used in the design and evaluation of experiments. The scientific questions formulated as hypotheses in the studies can be verified by the use of statistical tests. A nonparametric paired analysis, Wilcoxon Signed Rank Test, was used to test for differences between the materials (Paper I and II) and a nonparametric test, Mann–Whitney U test, was used for comparison between independent material groups (Paper II). Additionally, Spearman's rank correlation coefficient analysis was carried out to test the dependency between the expression levels of different genes in Paper II (SPSS 21, IBM, USA). In Paper III, linear regressions analysis was used to determine the effect of different variables on the torque response (MODDE 7.0.0.1, Umetrics AB, Sweden). A 0.05 level of significance was used in all statistical analysis.

4 SUMMARY OF RESULTS

4.1 Paper I

In this study the bone formation around and the anchorage of Zr doped Co–Cr–Mo implants fabricated by electron beam melting (Figure 6A and B) was evaluated *in vivo* after eight weeks of healing in rabbit. The established experimental model enables the analysis of both cortical and trabecular bone responses at the implant interface and in the peri-implant bone.

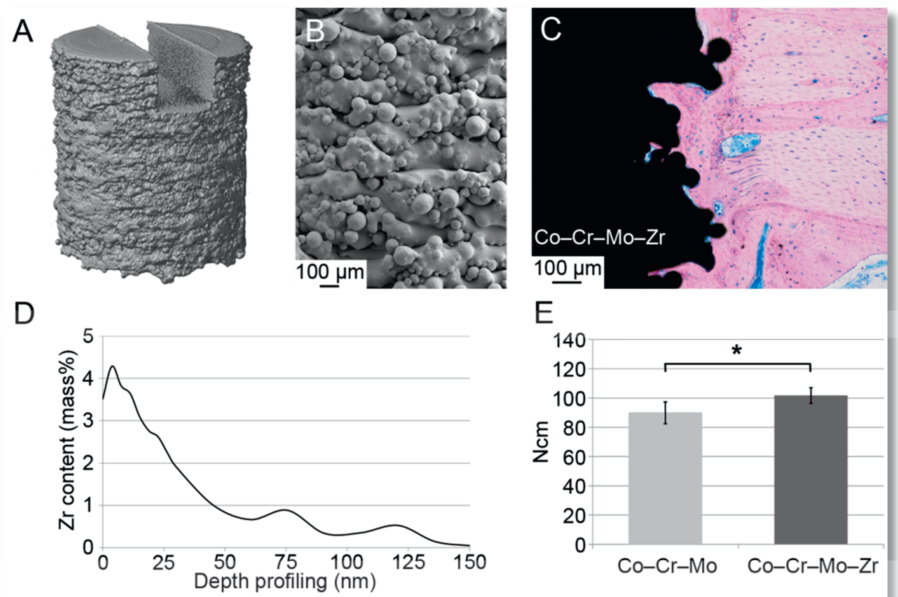

*Figure 6. A) A 3D rendering of the Co–Cr–Mo–Zr implant obtained by micro–CT. B) A scanning electron micrograph at 200× magnification of the Co–Cr–Mo–Zr implant surface, showing the surface morphology composed of a molten base with semi-molten beads with sizes of 30–100 µm. C) A light micrograph of the ground-section of a Co–Cr–Mo–Zr implant in the proximal position in the tibia. Bone ingrowth in the surface structures and in direct contact with the implant surface was observed. D) The amount of Zr in the Co–Cr–Mo–Zr implant along the depth profile, showing an enriched content of Zr at the surface. E) Mean values of the biomechanical data sets with standard error, n = 8 for each group. * Indicates significant difference (p < 0.05) using Wilcoxon Signed-Rank test.*

Qualitative histology revealed no apparent differences and both materials showed bone growing into surface irregularities and in direct contact with the material surface (Figure 6C). In addition, no adverse tissue reaction was observed. Areas of remodeling were observed both at a distance and in close proximity to the implant, with coupled osteoclastic and osteoblastic activity. The only significant difference in histomorphometry between the materials was observed for the Co–Cr–Mo implants in the tibia showing larger bone area at a distance from the implant surface.

The surface characterization revealed no significant differences in the surface topography with similar arithmetic mean height of the surface of about 10 µm. XPS analysis showed Cr and Mo oxides at the surface of both materials and an enrichment of Zr in the surface oxide compared to the bulk of the Zr doped material (Figure 6D).

Biomechanical analysis (removal torque) showed significantly higher implant stability for the Zr doped material after eight weeks healing compared with the Co–Cr–Mo (Figure 6E).

4.2 Paper II

In this study implants made of a novel Ti–Ta–Nb–Zr alloy (Figure 7A and C) were evaluated after 7 and 28 days of healing in a rat tibia model, with cp-Ti grade IV as reference material.

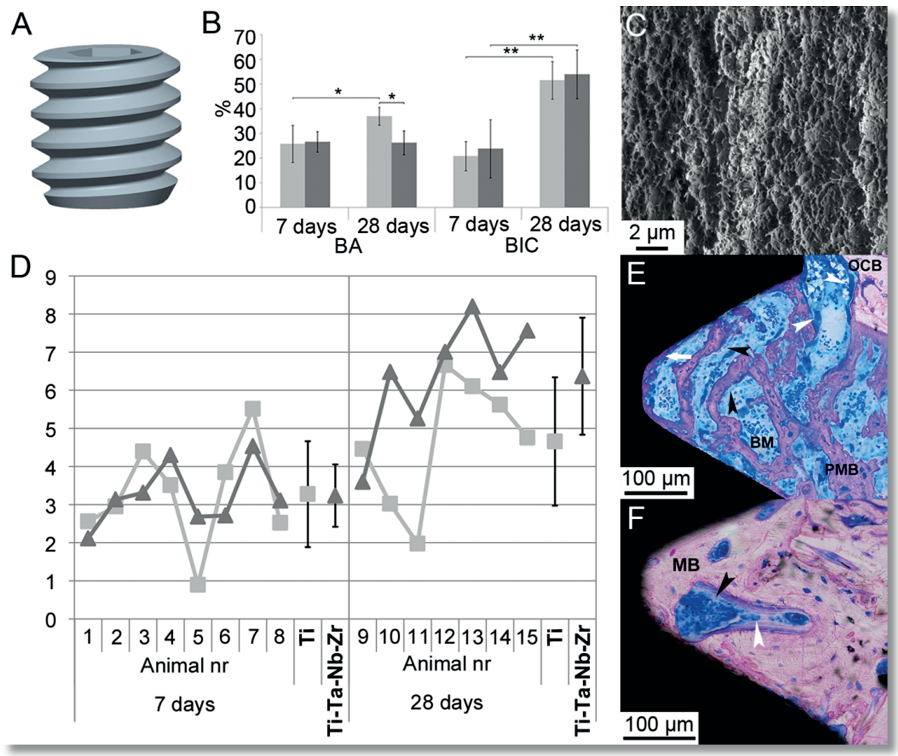

*Figure 7. A) A drawing of the implant design. B) The histomorphometry presented as mean bone area (BA) and mean bone-implant contact (BIC) within all the threads of each implant, Ti in light grey and Ti–Ta–Nb–Zr in dark grey. Significance $p < 0.05$ and $p < 0.001$ is indicated with * and **, respectively. N = 8 for both materials at both time points. C) A SEM micrograph in 10,000x magnification of the screw thread top surface of the Ti–Ta–Nb–Zr alloy. D) The maximum removal torque for the Ti implants (light-grey squares) and Ti–Ta–Nb–Zr implants (dark-grey triangles) measured at 7 and 28 days, presented with the mean for each material series at both evaluation times, indicated by a square or a triangle with standard deviation. N = 8 at 7 days and n = 7 at 28 days. E, F) Light micrographs of undecalcified ground sections of bone interface to Ti–Ta–Nb–Zr implants after 7 (E) and 28 (F) days' healing, respectively. OCB = original cortical bone, PMB = partially mineralized bone, BM = bone marrow, white arrow = osteoid, white arrowhead = osteoclast, black arrowhead = osteoblast seams.*

Surface characterization revealed a thin (<10 nm) surface oxide composed mainly of TiO_2, with enrichment of alloying elements at the top most surface. The Ti–Ta–Nb–Zr alloy showed similar surface wettability, cytotoxicity and surface roughness as the cp-Ti, but significant minor differences were detected for some roughness parameters.

Histomorphometry showed no difference in bone-implant contact between the materials at either time point. The Ti showed significantly higher bone area within the threads of the implant at the later time point compared with the Ti–Ta–Nb–Zr alloy (Figure 7B).

Measured removal torques revealed significantly increased implant stability over time for the Ti–Ta–Nb–Zr in contrast to the Ti. Still, no significant difference in stability was observed between the materials at either time point (Figure 7D).

The gene expression of the implant-adherent cells revealed about a 2-, 3- and 6-fold lower expression of pro-inflammatory (IL–1β and TNF–α), bone formation (Runx2 and OC) and bone remodeling (TRAP and CatK) genes at the Ti–Ta–Nb–Zr implants compared with the Ti ($p < 0.05$).

Furthermore, the histological and gene expression analyses suggested faster healing around the Ti–Ta–Nb–Zr, as judged by the enhanced mineralization and remodeling, of the early-formed woven bone and the multiple positive correlations between genes denoting inflammation, bone formation and remodeling.

In comparison with the clinically well-established pure Ti grade material, the novel alloy demonstrated equal cytocompatibility, induced less inflammatory response and became equally well osseointegrated (Figure 7E and F).

4.3 Paper III

In this study the effect of different factors on removal torque was identified by utilizing factorial experimental design. A bench model was developed where cylinders (Figure 8A) and threaded implants with modified surface roughness (Figure 8B–D) were embedded in different homogeneous thermosetting polymers and evaluated by removal torque analysis. This approach enables the study of different factors affecting the torque response without the influence of biological variability.

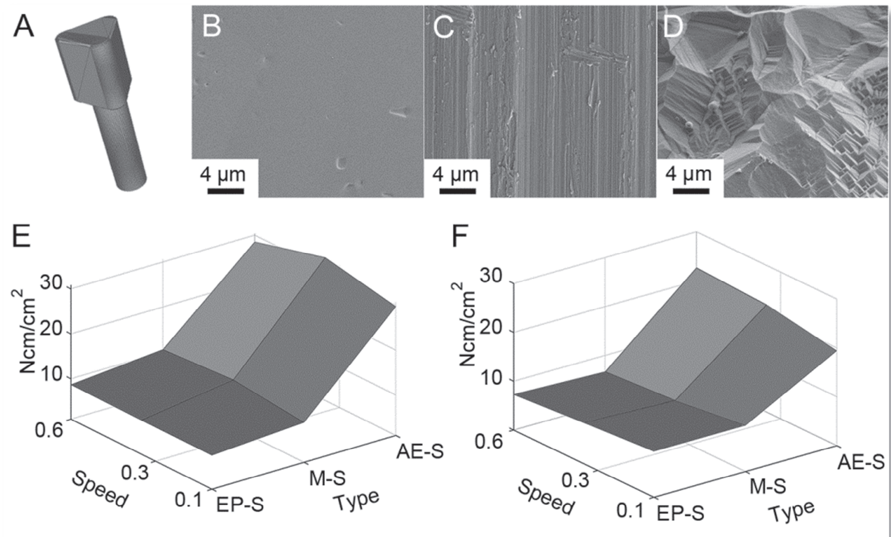

Figure 8. A) A drawing of the experimental cylinder. B, C, D) Micrographs of the experimental cylinder surface types: electropolished, EP (B), machined, M (C) and acid etched EA (D). E, F) Average maximum removal torque for spin-coated modified cylinders (n = 6) embedded in Altropol Multicast 30 (E) and Altropol EP 986 (F) thermosetting polymers.

It needs to be pointed out that the model represents a gross simplification as compared to the real *in vivo* situation and the results need to be validated against those of systematical removal torque studies *in vivo*. However, within the limit range of each factor studied the results showed that the maximum removal torque was significantly affected by the surface roughness and the surrounding material (Figure 8E and F). These factors were also found to demonstrate interplay between one another. The rotation speed was found not to influence the maximum removal torque. A gradual fracture progression of the interface was observed during the measurement starting from the top of the cylinder where the torque was applied, to the bottom.

4.4 Paper IV

In this study a 3-dimensional finite element model simulating the fracture progression at the implant interface during removal torque analysis was built based on details from Paper III. The approach comprised a macroscopic simulation of the interfacial response to the Ti cylinder when subjected to rotation and a microscopic simulation of the interfacial fracture progression at the interface between a conical Ti feature and the surrounding material (Figure 9A).

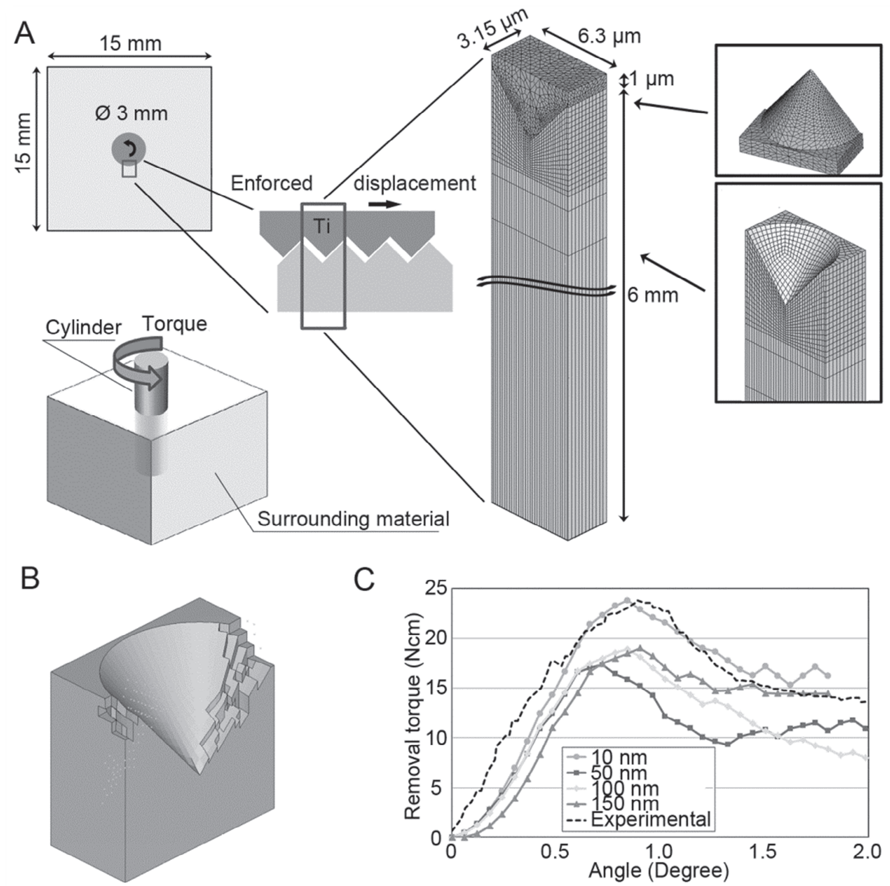

Figure 9. A) A schematic overview of the fracture model macro and micro geometries with the Ti cylinder in dark grey and the surrounding material in light grey. B) A cross-sectional view of the fractured surrounding material interface after six iterations for a gap size of 10 nm. C) Removal torque curves of the finite element analysis simulating different gap sizes in the interface region presented with one curve of the experimental bench study (Paper III).

The macroscopic model revealed a difference in displacement of 2.62 µm in total along the Ti interface when subjected to torque loads. This difference was later used when the results of the microscopic interface simulation were summed to determine the total response during displacement converted to torque vs angle.

The microscopic model showed a decreasing reaction force with increasing number of iterations over the same area. Introducing a gap at the interface was found to alter the fracture progression pattern (Figure 9B) resulting in altered torque responses. By combining the macro and micro models the results of the finite element analysis showed good agreement with the experimental results (Figure 9C). The model provides a possible explanation to how the fracture progression at the interface occurs, involving sequential fractures with loosening from the top of the implant to the bottom.

The shape of the retention element was found to influence the reaction force per unit area in the displacement direction. The reaction force per unit area for the evaluated shapes differed about 40% at the most and decreased in the following order: cuboid, turned cuboid, cylinder, pyramid, cone and turned pyramid. The contour plots of each retention element with surrounding material revealed stress concentrations at specific interfacial areas at the surface of both the feature and the surrounding material.

4.5 Paper V

In this study the bone responses to loading of trans-femoral amputation prostheses were evaluated. The results of site-specific loading measurements on amputees were used as input to finite element analyses (Figure 10A) simulating the stress and strain distributions in the bone tissue. Furthermore, a retrieved tissue sample from a patient undergoing implant revision was characterized in order to evaluate the long-term tissue response around the abutment.

The loading results revealed that the extreme loads varied among the patients as can be expected with respect to their individual anatomy, weight, amputation height and walking pattern.

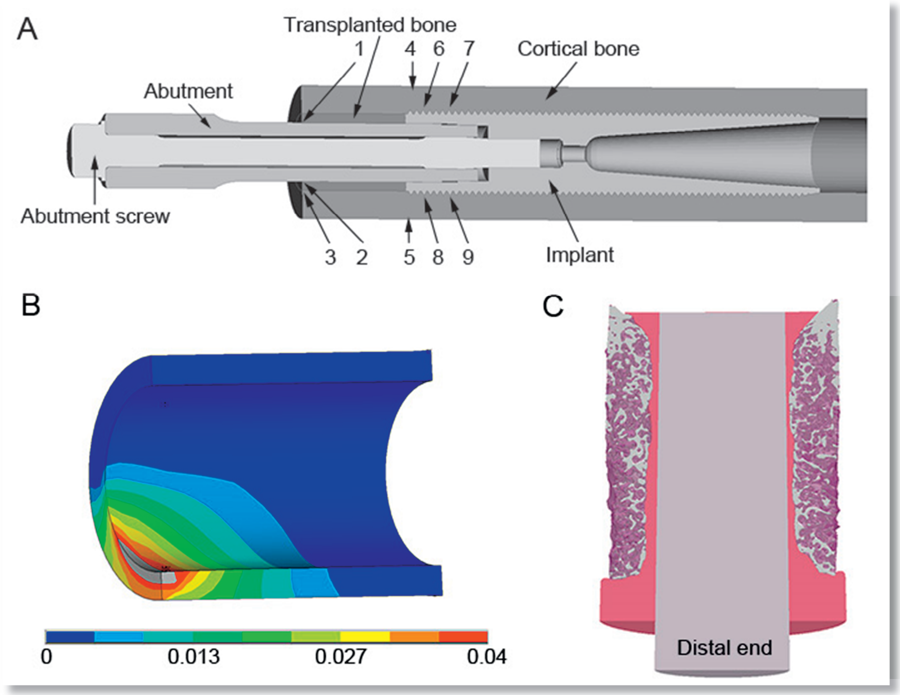

Figure 10. A) A cross-sectional schematic overview of the bone-implant-abutment-model design (M2, M3 and M4) with identified parts and bone regions as well as sites (1–9) of interest for the finite element analysis. B) The equivalent elastic strain distribution in the transplanted bone region) for a cross-section of the M2 model. C) A cross-sectional view of a µCT reconstruction of the transplanted bone region retrieved after 15 years in a patient. The segmented mineralized tissue (white), within the bone transplant region (purple), the soft tissue (red) and the assumed abutment (grey). The abutment was created and positioned centrally for analysis and visualization purposes.

The FEA showed that the loading caused the abutment to bend and displace the distal abutment end about 1 mm in total. At the same time a gap of between 0.06–0.14 mm was created between the bone and the abutment at the opposite side depending on the stiffness of the transplanted bone region. The highest shear stress levels were observed for the stiffest model with 4.0 MPa and 6.4 MPa at the interface between the cortical bone and the fixture in the 3rd and 7th thread, respectively. The same trend was observed for maximum principal stress levels in the most distal transplanted bone ranging between 22–77 MPa. The strain in the most distal cortical bone was 0.002–0.005 with higher strains for increasing overall model stiffness. The opposite was seen for the strain levels in the distal end of the transplanted bone region ranging between 0.018–0.06 with an increasing trend for decreasing stiffness (Figure 10B).

Micro–CT analysis of the tissue sample retrieved after 15 years *in vivo* revealed a densification in the region facing the abutment with more porous bone going radially outwards. The highest bone porosity was observed in between the proximal and distal end, with bone volume fractions of between 20–35%. The soft tissue between the bone and the abutment varied in thickness along the interface with a mean value of 0.94 mm (Figure 10C). These observations were later confirmed by qualitative and quantitative histology showing mean bone area of 28% and 36% for respective side of the evaluated specimen and a mean soft tissue thickness of 1.2 mm. The tissue facing the abutment mainly consisted of well vascularized granulation tissue with signs of inflammatory cell infiltrates in the distal region. Occasional bone resorption sites, with present osteoclasts, were observed in the bone side facing the abutment.

5 GENERAL DISCUSSION

Today, an implant is a commonly used treatment intended to restore a loss of function caused by disease or trauma. With increasing life expectancy and a growing elderly population as a result, more patients can be expected in the future. This creates a demand both for materials with improved strength suitable for implants with reduced dimensions, and to minimize the risk of mechanical failure in applications involving high loads. Furthermore, new implant designs, with structural stiffness similar to that of bone and with more optimal load distribution are needed, particularly in challenging clinical situations, such as compromised bone conditions. In addition, for these situations, implants with improved healing capacity are required in order to achieve necessary implant stability.

Additive manufacturing (AM) processes have gained considerable interest in recent years as technologies that offer unmatched freedom to design new implants. Complex open-cellular designs can be built that allow bone ingrowth which can improve the implant stability.[212] Additive manufacturing techniques have the possibility to be used for fabrication of e.g., knee and hip replacements which are truly patient-individualized. The capacity to process both Ti alloys and Co–Cr alloys makes electron beam melting (EBM) a promising AM technique for implant manufacturing in a variety of applications. Excellent results have already been observed for as-built Ti–6Al–4V structures *in vivo* in both rabbit and sheep studies,[178,179] as well as for acetabular cups in human.[212]

Material processing involves either thermal, mechanical, chemical treatment or a combination of these which will influence the final material properties and hence the biological response. Additionally, the material properties will directly influence the mechanical load distribution on the bone, which in turn affects the bone response, and hence the implant stability and clinical success. Surface properties play a particularly important role for medical implants. Commercially available implants show a wide variety of surface characteristics[99] and material properties. This makes identification of the effect of individual surface factors on the bone response and clinical performance difficult. And it emphasizes the need for systematical studies aiming to understand the underlying mechanisms and interface related factors responsible for specific responses.

5.1 Methodological considerations

Since no single surface characterization technique can provide all the desired information, several complementary techniques will have to be used in order to study both the structural and chemical aspects of the surface region of interest. The order of analysis needs to be planned since some techniques are destructive and might alter the properties to be subsequently analyzed. Additionally, parameters such as resolution, length scale, and penetration depth, as well as analysis area, need to be considered so that the chosen techniques fulfill the purpose of the analyses.

The analysis of the chemical composition of the implant material requires consideration of both the bulk and the surface. The latter is particularly important for biomedical implants since these are in direct contact with the biological environment. The relevant surface region typically corresponds to the topmost layers (<10 nm) and requires special techniques in order to be resolved from the rest of the material. Combining the XPS and the ICP–OES techniques enables comparison between the surface and the bulk composition, and is useful for investigating the influence of manufacturing and surface modification processes. However, it needs to be pointed out that XPS quantifies the relative elemental chemical composition of the material surface while the ICP–OES quantifies the absolute chemical composition averaged over the entire sample. XPS quantification of complex elemental compositions is associated with several challenges. It requires knowledge of the lateral and depth distribution as well as calibration against samples of known composition for accurate quantifications. In addition, analysis depth is element dependent and matrices with several different constituents can influence the calculations. Furthermore, contamination layers, such as hydrocarbons on the surface will also affect the results. Taken together, a relative error of at least 20–30% is not uncommon. Therefore the calculated concentrations should be considered as an average of the analyzed volume, and used mainly for comparison between different samples.

Characterization of the surface topography is associated with uncertainties related to both the surface properties and limitations of the applied technique. It is therefore recommended that several complementary techniques are used to characterize the topography adequately.[213] The surface topography is typically described by the form, waviness and the roughness of the surface and can consist of many different wavelengths that correspond to structures in the nm to mm range. Consequently, all wavelengths need to be described to fully characterize the surface topography and whenever the form, waviness or roughness is described the filter size used to separate them should be reported.[214] According to suggested guidelines, characterization should be made using different types of roughness parameters.[215]

There are several aspects that need to be taken under consideration when deciding which animal model to use; smaller animals like mice and rats have accelerated healing capacity compared to larger ones like rabbits and dogs. The implant size can be a decisive factor since limitations in the manufacturing process may require that larger animal models are used. From an ethical point of view the number of animals should be kept to a minimum which requires that the model, time points, number of samples and their placement are planned adequately, without compromising statistical power. Bone-anchored implants are typically evaluated with regard to their stability i.e., bone-implant interlocking at the interface. For evaluation of implants with screw shaped designs removal torque analysis is a useful method, where the torque required to break the interlocking is measured while subjecting the implant to a constant rotation. In order to fully understand the stability measurements the implant surface related factors need to be systematically investigated for each technique. Furthermore, characterization of the bone-implant interface helps to ensure that implants are correctly positioned in the bone, which otherwise most likely affects the measured stability.

Qualitative histology, quantitative histomorphometry and X–ray microtomography can be performed on the same retrieved sample and the combination of these techniques enables both 2- and 3-dimensional analysis of the bone-implant interface. Quantification of the bone-implant contact requires the interface to be intact and is therefore not possible after removal torque analysis which fractures the interface. The biological variability seen in animal studies can be a problem since it might exceed the effects under investigation. This requires comparison to be made within the individual animals, i.e. paired analyses. The relatively small sample sizes make it difficult to confirm normal distribution of the data, resulting in nonparametric testing. In correlation analysis the dependency between two variables is evaluated for which Pearson's correlation coefficient is most commonly used and describes the linear dependency, while Spearman's rank correlation coefficient describes how well the variables fit the response of a monotonic function. The latter is more suited for nonparametric distributions and hence used to analyze the correlation between the expression levels of different genes in Paper II.

Experimental bench models are particularly applicable in systematical evaluations of independent factors, such as mechanical retention that can be distinguished from biological responses. This approach eliminates the biological variation but is only valid within the limits of the evaluated factors and hence requires further *in vivo* validation. Experimental design can be used to further improve the precision of the results by identifying and reducing the sources of variability. Replicates should be used to strengthen the reliability and validity of the experiments and to avoid biases it is common practice to use randomization in the design. The main purpose of bone-anchored implants is to transfer loads to the skeleton. However, these loads can be difficult to determine due to inaccessibility of the implant site and ethical restrictions. Load-cell analyses are suitable given that the measurements can be completed without altering the loading situation.

5.2 Surface chemistry

The surface chemical composition is considered to be an important factor for the biological response and successful long-term treatment of osseointegrated prostheses. The materials need to be biocompatible and are generally selected based on the mechanical requirements of the intended application. For load-bearing, bone-anchored applications, metals are widely used, and some prefer Ti-based materials[68] while others prefer Co–Cr alloys.[182]

The modified Co–Cr–Mo alloy and the Ti–Ta–Nb–Zr alloy implants evaluated *in vivo* in Paper I and II, respectively showed comparable surface topography in terms of morphology and roughness compared with the corresponding controls. The surface chemical analysis revealed enrichment of the added alloying elements at the surface, compared to the bulk of both materials. These changes in chemical compositions seem to promote the formation of well mineralized bone tissue in direct contact with the implant as judged by histological results. Both materials showed equivalent levels of bone-implant contact as the control. However, significantly higher bone area was detected at a distance from the implant surface and within the implant threads of the controls for Paper I and II, respectively. Despite a lower bone amount, the Ti–Ta–Nb–Zr alloy showed comparable implant stability as the control after 7 and 28 days, with magnitudes in accordance with a previous study using a similar experimental model.[216] It can be hypothesized that the equal stability, despite less bone amount, could be due to faster bone remodeling and mineralization of the bone at the bone-implant interface. This was also indicated by the qualitative histological and gene expression analyses.

Both cp-Ti and Ti–6Al–4V are commonly used materials in bone-anchored implants with a proven clinical record. The latter material is selected where high load-bearing capacity is required. However, it remains to be determined, which of these materials is the better regarding the bone response. Concerns have been raised about the potential toxic effect of Al and V ions released *in vivo*. Even if no toxic levels were detected, elevated concentrations of V ions have been measured in kidney, lung and liver after 1 and 4 weeks in a study in rabbit.[217] The novel Ti–Ta–Nb–Zr alloy evaluated in Paper II showed no signs of cytotoxicity or adverse tissue reactions and became osseointegrated to a similar degree as the cp-Ti grade IV after 1 and 4 weeks *in vivo*. This agrees well with earlier reports on the biocompatibility of Ta, Nb and Zr in the literature.[188,218] The Zr–Nb–Ta alloyed Ti has been evaluated both *in vitro*[219] and *in vivo*[220] using a rat model and showed considerably lower metal release compared to 316L stainless steel, Co–Cr–Mo casting alloy, and Ti–6Al–4V. By replacing V with Nb the Ti–Al–Nb alloy has been shown to promote the cell-substrate interaction and activity *in vitro*, with increased cell attachment, proliferation and viability.[221] *In vitro* evaluation of the cellular response of human monocytes to wear particles from Co–Cr and Ti–Al–V prostheses showed that the former were very toxic while the latter induced more inflammatory mediators implicated in osteolysis.[65] The authors' opinion was that the release of Ti–Al–V particles would be worse than if equal amount of Co–Cr particles were to be released in the periprosthetic tissue. The number of bone-resorbing mediators released from cells was significantly reduced for Ti–Al–Nb compared with Ti–Al–V.[222] For unknown reasons the responses seen *in vitro* are typically not as pronounced *in vivo*. The excellent wear resistance of Co–Cr–Mo alloys[71] is an important property for joint implants, such as hip replacements.[182] These alloys possess high strength but have been regarded as inferior to Ti–6Al–4V in terms of bone anchorage.[197,198] Nevertheless, porous-coated Co–Cr hip stems showed excellent clinical results after two years when implanted with a tight press fit,[181] suggesting that the material could for be suitable also for cementless treatments.

Addition of Zr to the Co–Cr–Mo alloy proved to be beneficial for the bone response and bone anchorage in Paper I. The Zr-doped Co–Cr–Mo alloy showed increased implant stability compared with the control, which points towards a change in the bone quality that in turn may be attributed to the dissimilarity in surface chemistry. A similar response was recently reported for Zr doped Ti showing an increased implant stability compared with cp-Ti that was suggested to reflect an improved bone quality.[192] Zr implants showed in comparison to cp-Ti, a thicker amorphous layer at the ultrastructural level,[194] while a faster mineralization of the bone in the nearest vicinity of the implants was observed at the light microscopy level,[196] in a rabbit and a rat study, respectively. Ti–Zr alloys are currently used clinically with good osseointegration results and offer improved strength compared with conventional, cold worked, Ti grade IV.[223] Incorporation of Zr in the

Co–Cr–Mo alloy composition in Paper I, enhanced the implant stability in rabbit. Zirconium is an interesting material that shares several properties with Ti; they are found in the same row of the periodic table of the elements, both form stable oxides, and they both show biocompatibility[188] and the ability to achieve osseointegration.[194] The mechanisms underlying these differences in interfacial bone strength and quality are unknown but it could be hypothesized that the formation of a highly corrosion resistant stable oxide on the material surface[224] influences the ion release pattern of the material. *In vitro* studies have shown that low amounts of Zr added to Co–Cr alloys, can improve the cytocompatibility,[225] possibly due to reduced ion leakage of Co.[226] This is advantageous since Co ions have been shown to decrease the cell viability and cell proliferation *in vitro*.[227] This emphasizes the need for new alloys with equal biocompatibility and osseointegration ability with improved mechanical properties to meet the physical requirements of life-long clinical function.

5.3 Surface topography

Implant surface topography has previously been mentioned in the introduction and has been shown to affect mechanical retention, distribution and transfer of loads to the surrounding bone, as well as different biological aspects.[186] The topography is therefore crucial for the implant stability and clinical success. Surface treatments such as acid etching or anodization are commonly used to modify the surface topography of implants. Besides such intentional alteration of the surface roughness, these treatments are likely to change other surface properties like wettability or corrosion resistance.[72] In comparison to smooth surfaces, rougher ones expose a larger surface area to the biological environment. The effects of material chemistry are intensified due to the larger area, resulting in increased material surface interactions by the adsorption of mineral ions and biomolecules and possibly also adherent cells. The two different material surfaces treated by dual acid etching that were evaluated in Paper II, showed similar surface roughness and wettability, and achieved osseointegration and implant stability comparable with that seen in previous studies using roughened surfaces.[216,228]

Topography is typically categorized by the length scale of the surface features ranging from macro- to nanometer. Different aspects of the surface roughness can to some extent be numerically described by the size, shape and distribution of surface features. From a mechanical point of view, the surface roughness of bone-anchored implants can be altered to bring about a more even load distribution and an increase in the interfacial strength. The latter was shown in Paper III by using a polymer embedding approach eliminating the biological response and variability. The acid etched surface showed significantly different mechanical fixation compared with the machined or electropolished surface. When these surface types were evaluated with regard to their numerical roughness parameters, S_a and S_{dq} correlated with the maximum removal torque. These parameters have previously been identified as important and shown similar correlation trends in both theoretical and *in vivo* studies.[160,229] Furthermore, surface roughness has been shown to correlate with the amount of bone-implant contact, where surface treatments resulting in rougher surfaces were found advantageous.[163] Optimal roughness characteristics for bone applications have been proposed to be around 1.5 µm and 50% in terms of S_a and S_{dr}, respectively.[183] However, reality is not that simple, roughness needs to be characterized in more detail since one parameter cannot completely describe the surface. The use of individual surface roughness parameters as predictors for interfacial shear strength have shown limited use but a positive correlation between the theoretical shear strength and the size of a surface feature of the same shape has been reported.[157,158] Nanometer-scale topography has been shown to influence the biological response[184] but its influence on mechanical retention can be considered negligible in comparison to larger length-scales. Nanotopography is therefore not covered in this thesis, where all the evaluated implant surfaces showed submicron topography without any distinct nano-patterns.

The native design of EBM implants results in surface topographies about 10 to 50 times rougher than those that are typical for dental implants. It has proven difficult to accurately determine the surface roughness of as built EBM surfaces due to limitations of the measurement techniques. Their topography can be considered as intermediate macrostructures with sizes between those referred to as surface roughness and macrodesign. The topography evaluated in Paper I showed high secondary implant stability compared with the levels seen for implants with threaded designs evaluated using a similar model.[170] Estimation of the interfacial shear strength revealed levels several times greater for the EBM manufactured implants compared to levels reported for screw-shaped implants. The improved stability can be attributed to the interlocking of bone within the irregular implant surface topography, which is large enough to support the regeneration of osteonal bone structures. In comparison, the mechanical properties of the bone formed within the microtopography of for example commercial dental implants are most likely much lower, based on the prevention of crack propagation seen in lamellar bone structures.[230] The semi-spherical morphology resulting from the partially melted powder particles has been shown to promote cell attachment, proliferation, differentiation, and also allows bone ingrowth and mechanical interlocking.[146,176,177] Macrostructures in the range 25–300 µm have been evaluated in different *in vivo* studies and were shown to influence the bone formation and remodeling. [231-233] These studies showed faster woven bone formation within smaller structures while higher amount of lamellar bone was formed within structures larger than 140 µm compared with those of 100 µm and below. This indicates that the macrostructure of AM implants show great potential for load-bearing applications. However, their primary stability is yet to be determined.

The FEA evaluation of the fracture progression at the implants surface in Paper IV indicated that shear strength is influenced by the shape of retention elements i.e., topography. Microstructures consisting of densely packed pits of favorable shape and size have been proposed as potential candidates for improved shear strength in a theoretical model.[158] Furthermore, in non-contact situations where a gap is present at the interface between the implant surface and the bone, the simulations in Paper IV showed that the resulting fracture pattern and the shear strength was dependent on the gap size. This is relevant since the bone-implant contact usually has values below 100%. Taken together, the size, shape and distribution of the surface features, as well as the contact situation at the interface, influence the mechanical retention and hence implant fixation. Still, the interlocking is only as strong as the bone within the structure which emphasizes the importance that specific roughness characteristics need to be validated and systematically studied in more detail *in vivo,* in order to distinguish their individual effect from one another.

5.4 Loading conditions

Loading is vital for the maintenance of bone and a determining factor for changing the bone structure to achieve suitable load levels in the tissue. Identifying the mechanisms underlying these activities requires a thorough understanding of the load distribution in the tissue and the elicited cellular response. However, this has proven quite difficult due to the complex structure of bone and the variety seen in bones. Introducing implants complicate things even more, as the material, implant design and surface topography have all been shown to affect the load distribution.[207] Furthermore, the viscoelastic property of bone increases the functional stiffness of the implant interface when subjected to loading at high rates, which affects the way tissues perceive the load. Additive techniques enable the manufacturing of complex implant designs with integrated porosities that allow bone ingrowth and simultaneously reduce the structural stiffness of the implant which results in more bone-like deformations.

The extreme loads applied on the amputation prosthesis during walking in Paper V resulted in stress concentrations at the cortical bone-fixture interface. The estimated shear stress levels were generally below the reported limit for shear loosening[128] even though separation may have occurred in some regions. This agrees well with the clinical observations where stable fixations have been confirmed up to 10 years after implantation.[111] Loading is a prerequisite for long-term success of implants since it serves as a stimulus for bone modeling and remodeling to achieve the necessary implant stability via architectural alterations. This concept originates from Wolff back in the 19th century and constitutes the current basis for the adaptive response of bone. The estimated stress and strain levels in the cortical bone in Paper V, were below previously reported yield and ultimate strength limits,[26,27] but reaching levels suitable for bone maintenance. This is in accordance with radiographic follow-ups of that bone region, showing no signs of bone resorption.[111] However, this was not the case for the transplanted bone in Paper V, where the stress and strain levels simulated by FEA were above the yield limit in the most distal region facing the abutment. These levels were likely to cause bone damage with subsequent bone remodeling. Histological analysis of this bone region retrieved from a patient after 15 years (Paper V), revealed occasional fractures of thin trabecula and ongoing bone remodeling. Additionally, the bone closest to the abutment was resorbed and had been replaced by soft tissue with an average thickness of 1.2 mm, possibly due to relative motions between the bone and the abutment.[78,79]

Different loading conditions, such as frequency, rate, duration, magnitude and recovery time, as well as direction, have been thought to play a role in bone responses.[21] The results presented in the literature indicate that more than one of these factors can induce a bone response given the right settings.[234] High static strains achieved by press-fit i.e., implants with oversized diameters, were shown to result in higher primary implant stability that remained throughout the observation time of 24 days *in vivo* (rabbit).[235,236] However, long-term studies are still lacking. The induced static strains caused microcracks in the tissue but did not trigger extensive bone remodeling or compression necrosis as previously been seen by others.[237] The bone seems to be somewhat insensitive to duration once a certain threshold or response been reached.[238] The sample retrieved in Paper V revealed a densification of the remaining bone facing the abutment when evaluated by μCT. This single case evaluation supports the findings of the FEA where the bone closest to the abutment and subjected to the highest loads is likely to fracture and undergo remodeling, with a net bone resorption over time until equilibrium is reached. In order to identify the local mechanisms behind such structural changes, the mechanics of individual bone structures and their effect on one another when assembled to a complete bone need to be considered. As observed in load-cell measurements in Paper V, the patients showed different load magnitudes and unique loading patterns. Additionally, the mechanical conditions in the bone tissue were likely to turn out differently due to their individual anatomy. Consequently, the optimal loading to generate the most appropriate stimuli for the cells under the reigning circumstances can be expected to vary, depending on the interfacial condition.

5.5 Implant stability

The factors influencing implant stability are the surface topography at different length scales, the bone-implant interface condition, and the properties of the surrounding bone. The latter two factors are interconnected and will affect one another. They are also affected by the surface topography both by its effect on cellular responses and by alteration of the load distribution around the implant. Hence, surface topography can have effects on the bone modeling and remodeling. Both the chemical composition of the implant surface, the contact situation, and the mechanical conditions are important for the bone response and fixation of the implant necessary for long-term clinical success. The initial contact situation is determined by the bone anatomy, implant design, and the surgical protocol and precision. These factors are important for achieving high primary implant stability and to avoid causing excessive damage to the bone tissue. Evaluation of implant stability by removal torque analysis provides insight into the mechanical load this specific bone-implant interface can withstand before fracture. Maximum removal torque values reported in literature show a quite wide spread, but caution should be taken when comparing results from different studies. Instead, interfacial shear strength may be a more relevant quantity for comparison. By combining the measured torques with the distance from the center axis to the surface of the implant (implant radius) and the surface area in contact with bone, one can estimate the interfacial shear strength. Taking the amount of bone interlocked within the surface retention elements into account in turn reflects the bone quality, i.e. its mechanical strength which varies with composition and structural organization. This is recommended when comparing results from different studies, where different implant dimensions, surface properties and animal models have been used.

6 CONCLUSION OF THE THESIS

The main findings and conclusions of this thesis are the following:

- The Co–Cr–Mo alloy implants manufactured by electron beam melting were found to osseointegrate in an *in vivo* rabbit model. Addition of 0.04 wt% Zr to the alloy further enhanced the implant stability.

- A novel Ti–Ta–Nb–Zr alloy became osseointegrated to a similar degree as cp-Ti implants. The alloy showed indications of faster bone healing than the pure Ti. After further optimization of the mechanical properties this alloy has the potential to serve as a new implant material for challenging applications, such as small-diameter implants and/or high-load-bearing prostheses.

- Within the limit range evaluated in the bench model experiments, the surface topography (surface roughness) as well as the medium surrounding an implant was found to significantly influence implant stability measured by removal torque. These results were later supported by finite element simulations. The developed finite element model provided a plausible explanation to the fracture progression at an implant interface.

- The loads applied on an osseointegrated amputation prosthesis in human were successfully determined by site-specific load cell measurements on several patients. Finite element analysis indicated that the loads may compromise the sealing function around the abutment, are likely to induce bone resorption of the transplanted bone at the most distal end, and induce bone adaption by new bone formation in the cortical bone. This was supported by results from µCT and histological analysis of a single retrieved tissue sample.

In summary, a combination of methods ranging from material processing and characterization, bench tests, *in vivo* evaluation, finite element simulations, and investigation on clinical material made it possible to systematically study the effects of specific factors on implant stability. It was concluded that the surface topography, the surface chemistry and the medium surrounding the implant were all found to influence the stability of the implant. A model of interfacial retention and fracture progression around an implant was proposed. Observations of bone resorption around an amputation abutment can partly be explained by the long-term effect of daily loading.

7 FUTURE PERSPECTIVES

The findings of this thesis demonstrate the importance of both surface topography for implant fixation and surface chemistry for the bone healing around implants and thus on the implant stability. Therefore it would be of interest to further explore the following:

- The theories formulated in the experimental studies of the thesis *in vivo,* in order to validate the results and to discriminate between the effects of the discussed factors on implant stability. This is a prerequisite to fully understand implant stability and how to optimize each factor in order to achieve an ideal response.

- Novel materials, like the Ti–Ta–Nb–Zr alloy, with potential to be used in challenging clinical applications and to further optimize the mechanical properties.

- More complex models, mimicking the physiological geometry and the anisotropic mechanical properties of bone in finite element modeling. Patient specific models with estimated bone mineral density can be built by e.g. μCT reconstructions and available advanced software.

- The microbiology and the tissue response to loaded transcutaneous implants in humans.

I believe that when a deeper understanding of how to optimize implants with regard to material, design, surface properties and mechanical stimuli in order to achieve desired tissue responses, patient unique solutions will overcome the most challenging clinical situations.

ACKNOWLEDGEMENT

I am fortunate to have been part of such inspirational interdisciplinary collaborations and would like to express my sincere gratitude to everyone who has contributed to this thesis.

First and foremost, I would like to thank my main supervisor Anders Palmquist for your encouragement and guidance throughout these years. You always made time to discuss everything from science to life itself. I am forever grateful for your support.

My deepest gratitude to my co-supervisors Jukka Lausmaa and Peter Thomsen who provided me with the opportunity to perform research within the field of biomaterial and allowing me to pursue my ideas. Jukka, your technical expertise and broad perspectives were always highly appreciated. Thanks Peter for sharing your profound knowledge in medicine and biology.

Thanks to my boss Benny Lyvén for your open-heartedness, support and the opportunity to work in challenging projects and be part of the future.

Thanks to my mentor, Rickard Brånemark, for sharing your mechanical understanding and involving me in inspiring collaborations.

My sincere gratitude to Kohei Murase for fruitful collaboration and many late-night Skype sessions on the topic of complex finite element analysis.

The warmest appreciation to my co-authors; Omar Omar, Felicia Suska, Margarita Trobos, Birgitta Norlindh, Anna Johansson, Ulrika Brohede, Susanne Norgren, Christina Stålhandske, Akihiko Chiba, Shingo Kuroso, Kota Takayanagi, Hiroaki Matsumoto, Yuichiro Koizumi and Akira Nakata for your surgical skillfulness, laboratory assistance, FEA and valuable input to the scientific papers.

The deepest thanks to all laboratory personnel at the department of Biomaterial at University of Gothenburg, especially Lena Emanuelsson, Birgitta Norlindh, Anna Johansson and Maria Hoffman for your excellent technical assistance during surgery, histological preparation and kindness.

I would also like to thank Eva Häggström, Roy Tranberg and Roland Zügner at Lundberg Laboratory for Orthopedic Research at Sahlgrenska University

Hospital for their support during biomechanical measurements. Mats Johansson and Camilla Knifsund at Uniso Technologies AB for their mechanical expertise and finite element analyses, Katarzyna Kulbacka-Ortiz at Sahlgrenska University Hospital for her assistance with patent related information, all the colleagues involved in the BIOMATCELL project.

I am grateful to all my former and present colleagues at the Department of Chemistry, Materials and Surfaces at SP Technical Research Institute of Sweden and the Department of Biomaterials at University of Gothenburg for assisting me during my journey and creating an inspiring and pleasant working environment. A special thanks to Annika Juhlin for proofreading the thesis.

Thomas thanks for believing in me and my research, for that I am forever grateful, rest in peace.

Finally, I would like to express my gratitude to my friends and family for your love and support. Mom and dad thank you for everything, for your unconditional support and encouragement through life which made this possible.

To Karin my love and light for always being there when needing you the most!

The present study was made in collaboration between SP Technical Research Institute of Sweden and the Department of Biomaterials, Institute of Clinical Sciences, Sahlgrenska Academy at University of Gothenburg.

Financial support was received from the BIOMATCELL VINN Excellence Center of Biomaterials and Cell Therapy, VINNOVA, VINNOVA-JSPS, BIOSUM, the Region Västra Götaland, the Swedish Research Council (grant K2015-52X-09495-28-4), SP Competence Platform Medtech, ALF/LUA grant (ALFGBG- 138721), the Area of Advance Materials of Chalmers and GU Biomaterials within the Strategic Research Area initiative launched by the Swedish Government, the IngaBritt and Arne Lundberg Foundation, Wilhelm and Martina Lundgren Foundation, the Dr. Felix Neubergh Foundation, Promobilia, the Adlerbertska Foundation, the Hjalmar Svensson Foundation, the Kungl och Hvitfeldtska Foundation and the Sahlgrenska Academy at University of Gothenburg, the Regional Innovation Cluster Program 2010, a grant-in-aid for Scientific Research Development, the Cooperation of Innovative Technology and Advanced Research in Evolving Area from MEXT and a grant-in-aid from the JSPS.

REFERENCES

1. Buckwalter JA, Glimcher MJ, Cooper RR, Recker R. Bone biology. I: Structure, blood supply, cells, matrix, and mineralization. *Instr. Course Lect.* 1996;45:371.
2. Mackie EJ. Osteoblasts: novel roles in orchestration of skeletal architecture. *Int. J. Biochem. Cell Biol.* 2003;35(9):1301-1305.
3. Raisz LG, Kream BE. Regulation of Bone Formation. *N. Engl. J. Med.* 1983;309(1):29-35.
4. Charles JF, Aliprantis AO. Osteoclasts: more than 'bone eaters'. *Trends Mol. Med.* 2014;20(8):449-459.
5. Manolagas SC. Birth and death of bone cells: basic regulatory mechanisms and implications for the pathogenesis and treatment of osteoporosis. *Endocr. Rev.* 2000;21(2):115-137.
6. Skerry TM, Bitensky L, Chayen J, Lanyon LE. Early strain-related changes in enzyme activity in osteocytes following bone loading in vivo. *Journal of bone and mineral research : the official journal of the American Society for Bone and Mineral Research.* 1989;4(5):783.
7. Cowin SC, Moss-Salentijn L, Moss ML. Candidates for the Mechanosensory System in Bone. *J. Biomech. Eng.* 1991;113(2):191-197.
8. Cowin SC. Bone poroelasticity. *J. Biomech.* 1999;32(3):217-238.
9. Mullender MG, Huiskes R. Osteocytes and bone lining cells: Which are the best candidates for mechano-sensors in cancellous bone? *Bone.* 1997;20(6):527-532.
10. Everts V, Delaissé JM, Korper W, et al. The Bone Lining Cell: Its Role in Cleaning Howship's Lacunae and Initiating Bone Formation. *J. Bone Miner. Res.* 2002;17(1):77-90.
11. Clarke B. Normal Bone Anatomy and Physiology. *Clin. J. Am. Soc. Nephrol.* 2008;3(Supplement 3):S131-S139.
12. Stock SR. The Mineral-Collagen Interface in Bone. *Calcif. Tissue Int.* 2015 [Epub ahead of print].
13. Whitehouse WJ, Dyson ED. Scanning electron microscope studies of trabecular bone in the proximal end of the human femur. *J. Anat.* 1974;118(Pt 3):417-444.
14. Larsson C, Esposito M, Liao H, Thomsen P. The Titanium-Bone Interface In Vivo. *Titanium in Medicine*: Springer Berlin Heidelberg; 2001:587-648.
15. Gerstenfeld LC, Cullinane DM, Barnes GL, Graves DT, Einhorn TA. Fracture healing as a post-natal developmental process: Molecular, spatial, and temporal aspects of its regulation. *J. Cell. Biochem.* 2003;88(5):873-884.
16. Ferguson C, Alpern E, Miclau T, Helms JA. Does adult fracture repair recapitulate embryonic skeletal formation? *Mech. Dev.* 1999;87(1–2):57-66.
17. Bilezikian JP, Raisz LG, Rodan GA. *Principles of bone biology.* San Diego, Calif: Academic Press; 2002.
18. Seeman E, Delmas PD. MECHANISMS OF DISEASE: Bone Quality - The Material and Structural Basis of Bone Strength and Fragility. *The New England journal of medicine.* 2006;354(21):2250.

19. Sims NA, Martin TJ. Coupling the activities of bone formation and resorption: a multitude of signals within the basic multicellular unit. *BoneKEy Reports.* 2014;3:481.
20. Teti A. Mechanisms of osteoclast-dependent bone formation. *BoneKEy Reports.* 2013;2:449.
21. Turner CH. Skeletal Adaptation to Mechanical Loading. *Clinical Reviews in Bone and Mineral Metabolism.* 2007;5(4):181-194.
22. Kini U, Nandeesh BN. Physiology of Bone Formation, Remodeling, and Metabolism. In: Fogelman I, Gnanasegaran G, van der Wall H, eds. *Radionuclide and Hybrid Bone Imaging*: Springer Berlin Heidelberg; 2012:29-57.
23. Lotz JC, Gerhart TN, Hayes WC. Mechanical properties of metaphyseal bone in the proximal femur. *J. Biomech.* 1991;24(5):317-329.
24. Turner CH. Bone strength: current concepts. *Ann. N. Y. Acad. Sci.* 2006;1068:429-446.
25. Rho J-Y, Kuhn-Spearing L, Zioupos P. Mechanical properties and the hierarchical structure of bone. *Med. Eng. Phys.* 1998;20(2):92-102.
26. Yamada H, Gaynor Evans F. *Strength of biological materials.* Baltimore: Williams & Wilkins; 1970.
27. Reilly DT, Burstein AH. The elastic and ultimate properties of compact bone tissue. *J. Biomech.* 1975;8(6):393-405.
28. Cowin SC. Mechanical modeling of the stress adaptation process in bone. *Calcif. Tissue Int.* 1984;36 Suppl 1:S98-103.
29. Mellon SJ, Tanner KE. Bone and its adaptation to mechanical loading: A review. *Int. Mater. Rev.* 2012;57(5):235-255.
30. Mosley JR, Lanyon LE. Strain rate as a controlling influence on adaptive modeling in response to dynamic loading of the ulna in growing male rats. *Bone.* 1998;23(4):313-318.
31. Linde F, Nørgaard P, Hvid I, Odgaard A, Søballe K. Mechanical properties of trabecular bone. Dependency on strain rate. *J. Biomech.* 1991;24(9):803-809.
32. Qin YX, Rubin CT, McLeod KJ. Nonlinear dependence of loading intensity and cycle number in the maintenance of bone mass and morphology. *J. Orthop. Res.* 1998;16(4):482-489.
33. Turner CH, Owan I, Takano Y. Mechanotransduction in bone: role of strain rate. *Am. J. Physiol.* 1995;269(3 Pt 1):E438-442.
34. Carter DR. The relationship between in vivo strains and cortical bone remodeling. *Crit. Rev. Biomed. Eng.* 1982;8(1):1-28.
35. De Smet E, Jaecques SV, Jansen JJ, Walboomers F, Vander Sloten J, Naert IE. Effect of constant strain rate, composed of varying amplitude and frequency, of early loading on peri-implant bone (re)modelling. *J. Clin. Periodontol.* 2007;34(7):618-624.
36. Fung YC. *Biomechanics: Mechanical Properties of Living Tissues.* 2 ed: Springer-Verlag New York; 1993.
37. Choi K, Kuhn JL, Ciarelli MJ, Goldstein SA. The elastic moduli of human subchondral, trabecular, and cortical bone tissue and the size-dependency of cortical bone modulus. *J. Biomech.* 1990;23(11):1103-1113.

38. Goldstein SA. The mechanical properties of trabecular bone: dependence on anatomic location and function. *J. Biomech.* 1987;20(11-12):1055-1061.
39. Zimmermann EA, Schaible E, Bale H, et al. Age-related changes in the plasticity and toughness of human cortical bone at multiple length scales. *Proceedings of the National Academy of Sciences.* 2011;108(35):14416-14421.
40. McCalden RW, McGeough JA, Barker MB, Court-Brown CM. Age-related changes in the tensile properties of cortical bone. The relative importance of changes in porosity, mineralization, and microstructure. *J. Bone Joint Surg. Am.* 1993;75(8):1193-1205.
41. Chen H, Zhou X, Fujita H, Onozuka M, Kubo K-Y. Age-Related Changes in Trabecular and Cortical Bone Microstructure. *International Journal of Endocrinology.* 2013;2013:213234.
42. Linde F, Hvid I, Madsen F. The effect of specimen geometry on the mechanical behaviour of trabecular bone specimens. *J. Biomech.* 1992;25(4):359-368.
43. Rice JC, Cowin SC, Bowman JA. On the dependence of the elasticity and strength of cancellous bone on apparent density. *J. Biomech.* 1988;21(2):155-168.
44. Ciarelli MJ, Goldstein SA, Kuhn JL, Cody DD, Brown MB. Evaluation of orthogonal mechanical properties and density of human trabecular bone from the major metaphyseal regions with materials testing and computed tomography. *J. Orthop. Res.* 1991;9(5):674-682.
45. Burstein AH, Reilly DT, Martens M. Aging of bone tissue: mechanical properties. *J. Bone Joint Surg. Am.* 1976;58(1):82-86.
46. Reilly DT, Burstein AH, Frankel VH. The elastic modulus for bone. *J. Biomech.* 1974;7(3):271-275.
47. Wertheim G. Memoire sur l'elasticité et la cohésion des principaux tissus du corps humain. *Ann. Chim. Phys.* 1847;21:385-414.
48. Lakes RS, Katz JL. Viscoelastic properties of wet cortical bone--II. Relaxation mechanisms. *J. Biomech.* 1979;12(9):679-687.
49. Carter DR, Caler WE, Spengler DM, Frankel VH. Fatigue behavior of adult cortical bone: the influence of mean strain and strain range. *Acta Orthop. Scand.* 1981;52(5):481-490.
50. Lee TC, Mohsin S, Taylor D, et al. Detecting microdamage in bone. *J. Anat.* 2003;203(2):161-172.
51. Carter DR, Hayes WC. Compact bone fatigue damage: a microscopic examination. *Clin. Orthop. Relat. Res.* 1977(127):265-274.
52. Vashishth D, Tanner KE, Bonfield W. Contribution, development and morphology of microcracking in cortical bone during crack propagation. *J. Biomech.* 2000;33(9):1169-1174.
53. Vashishth D, Tanner KE, Bonfield W. Experimental validation of a microcracking-based toughening mechanism for cortical bone. *J. Biomech.* 2003;36(1):121-124.
54. Lee TC, Staines A, Taylor D. Bone adaptation to load: microdamage as a stimulus for bone remodelling. *J. Anat.* 2002;201(6):437-446.

55. Carter DR. Mechanical loading histories and cortical bone remodeling. *Calcif. Tissue Int.* 1984;36 Suppl 1:S19-24.
56. Mori S, Burr DB. Increased intracortical remodeling following fatigue damage. *Bone.* 1993;14(2):103-109.
57. Athanasiou KA, Zhu C, Lanctot DR, Agrawal CM, Wang X. Fundamentals of biomechanics in tissue engineering of bone. *Tissue Eng.* 2000;6(4):361-381.
58. Turner CH, Burr DB. Basic biomechanical measurements of bone: a tutorial. *Bone.* 1993;14(4):595-608.
59. Frost HM. From Wolff's law to the Utah paradigm: insights about bone physiology and its clinical applications. *Anat. Rec.* 2001;262(4):398-419.
60. Williams DF, Biomaterials ESf. *Definitions in Biomaterials: Proceedings of a Consensus Conference of the European Society for Biomaterials, Chester, England, March 3-5, 1986.* Elsevier; 1987.
61. Branemark PI, Hansson BO, Adell R, et al. Osseointegrated implants in the treatment of the edentulous jaw. Experience from a 10-year period. *Scand. J. Plast. Reconstr. Surg. Suppl.* 1977;16:1-132.
62. Dorland WAN. *Dorland's illustrated medical dictionary.* Philadelphia, Pa: Elsevier/Saunders; 2012.
63. Navarro M, Michiardi A, Castaño O, Planell JA. Biomaterials in orthopaedics. *J. Royal Soc. Interface.* 2008;5(27):1137-1158.
64. Long M, Rack HJ. Titanium alloys in total joint replacement—a materials science perspective. *Biomaterials.* 1998;19(18):1621-1639.
65. Haynes DR, Rogers SD, Hay S, Pearcy MJ, Howie DW. The Differences in Toxicity and Release of Bone-Resorbing Mediators Induced by Titanium and Cobalt-Chromium-Alloy Wear Particles. *J. Bone Joint Surg. Am.* 1993;75A(6):825-834.
66. Hanawa T. 1 - Overview of metals and applications. In: Niinomi M, ed. *Metals for Biomedical Devices*: Woodhead Publishing; 2010:3-24.
67. Bobyn JD, Glassman AH, Goto H, Krygier JJ, Miller JE, Brooks CE. The effect of stem stiffness on femoral bone resorption after canine porous-coated total hip arthroplasty. *Clin. Orthop. Relat. Res.* 1990(261):196-213.
68. Head WC, Bauk DJ, Emerson RH, Jr. Titanium as the material of choice for cementless femoral components in total hip arthroplasty. *Clin. Orthop. Relat. Res.* 1995(311):85-90.
69. Rack HJ, Qazi JI. Titanium alloys for biomedical applications. *Materials Science & Engineering C-Biomimetic and Supramolecular Systems.* 2006;26(8):1269-1277.
70. Niinomi M. Mechanical biocompatibilities of titanium alloys for biomedical applications. *J. Mech. Behav. Biomed. Mater.* 2008;1(1):30-42.
71. Tkachenko S, Datskevich O, Kulak L, Jacobson S, Engqvist H, Persson C. Wear and friction properties of experimental Ti-Si-Zr alloys for biomedical applications. *J. Mech. Behav. Biomed. Mater.* 2014;39:61-72.
72. Liu X, Chu PK, Ding C. Surface modification of titanium, titanium alloys, and related materials for biomedical applications. *Materials Science and Engineering: R: Reports.* 2004;47(3–4):49-121.

73. Saldivar-Garcia AJ, Lopez HF. Microstructural effects on the wear resistance of wrought and as-cast Co-Cr-Mo-C implant alloys. *J. Biomed. Mater. Res. A.* 2005;74(2):269-274.
74. Sun S-H, Koizumi Y, Kurosu S, Li Y-P, Matsumoto H, Chiba A. Build direction dependence of microstructure and high-temperature tensile property of Co–Cr–Mo alloy fabricated by electron beam melting. *Acta Mater.* 2014;64:154–168.
75. Kuzyk PR, Schemitsch EH. The basic science of peri-implant bone healing. *Indian journal of orthopaedics.* 2011;45(2):108-115.
76. Davies JE. Understanding peri-implant endosseous healing. *J. Dent. Educ.* 2003;67(8):932.
77. Palmquist A, Omar OM, Esposito M, Lausmaa J, Thomsen P. Titanium oral implants: surface characteristics, interface biology and clinical outcome. *J. R. Soc. Interface.* 2010;7 Suppl 5:S515-527.
78. Pilliar RM, Lee JM, Maniatopoulos C. Observations on the effect of movement on bone ingrowth into porous-surfaced implants. *Clin. Orthop.* 1986(208):108.
79. Szmukler-Moncler S, Salama H, Reingewirtz Y, Dubruille JH. Timing of loading and effect of micromotion on bone-dental implant interface: review of experimental literature. *J. Biomed. Mater. Res.* 1998;43(2):192-203.
80. Parel SM, Branemark PI, Jansson T. Osseointegration in Maxillofacial Prosthetics .1. Intraoral Applications. *J. Prosthet. Dent.* 1986;55(4):490-494.
81. Parel SM, Branemark PI, Tjellstrom A, Gion G. Osseointegration in Maxillofacial Prosthetics .2. Extraoral Applications. *J. Prosthet. Dent.* 1986;55(5):600-606.
82. Branemark R, Berlin O, Hagberg K, Bergh P, Gunterberg B, Rydevik B. A novel osseointegrated percutaneous prosthetic system for the treatment of patients with transfemoral amputation: A prospective study of 51 patients. *The bone & joint journal.* 2014;96-B(1):106-113.
83. Holgers K-M, Esposito M, Källtorp M, Thomsen P. Titanium in Soft Tissues. *Titanium in Medicine*: Springer Berlin Heidelberg; 2001:513-560.
84. von Recum AF. Applications and failure modes of percutaneous devices: a review. *J. Biomed. Mater. Res.* 1984;18(4):323.
85. Astrand P, Ahlqvist J, Gunne J, Nilson H. Implant treatment of patients with edentulous jaws: a 20-year follow-up. *Clin. Implant Dent. Relat. Res.* 2008;10(4):207-217.
86. Lekholm U, Grondahl K, Jemt T. Outcome of oral implant treatment in partially edentulous jaws followed 20 years in clinical function. *Clin. Implant Dent. Relat. Res.* 2006;8(4):178-186.
87. Adell R, Eriksson B, Lekholm U, Branemark PI, Jemt T. Long-term follow-up study of osseointegrated implants in the treatment of totally edentulous jaws. *Int. J. Oral Maxillofac. Implants.* 1990;5(4):347-359.
88. Sennerby L, Ericson LE, Thomsen P, Lekholm U, Astrand P. Structure of the bone-titanium interface in retrieved clinical oral implants. *Clin. Oral Implants Res.* 1991;2(3):103-111.
89. Jaffin RA, Berman CL. The Excessive Loss of Branemark Fixtures in Type IV Bone: A 5-Year Analysis. *J. Periodontol.* 1991;62(1):2-4.

90. Greenstein G, Cavallaro J, Romanos G, Tarnow D. Clinical recommendations for avoiding and managing surgical complications associated with implant dentistry: a review. *J. Periodontol.* 2008;79(8):1317-1329.
91. Listgarten MA, Lang NP, Schroeder HE, Schroeder A. Periodontal tissues and their counterparts around endosseous implants [corrected and republished with original paging, article orginally printed in Clin Oral Implants Res 1991 Jan-Mar;2(1):1-19]. *Clin. Oral Implants Res.* 1991;2(3):1-19.
92. Quirynen M, Bollen CM. The influence of surface roughness and surface-free energy on supra- and subgingival plaque formation in man. A review of the literature. *J. Clin. Periodontol.* 1995;22(1):1.
93. Stanford CM, Schneider GB. Functional behaviour of bone around dental implants. *Gerodontology.* 2004;21(2):71-77.
94. Duyck J, Naert IE, Van Oosterwyck H, et al. Biomechanics of oral implants: a review of the literature. *Technol. Health Care.* 1997;5(4):253-273.
95. Tolstunov L. Dental implant success-failure analysis: a concept of implant vulnerability. *Implant Dent.* 2006;15(4):341-346.
96. Tada S, Stegaroiu R, Kitamura E, Miyakawa O, Kusakari H. Influence of implant design and bone quality on stress/strain distribution in bone around implants: a 3-dimensional finite element analysis. *Int. J. Oral Maxillofac. Implants.* 2003;18(3):357-368.
97. Hart RT, Hennebel VV, Thongpreda N, Van Buskirk WC, Anderson RC. Modeling the biomechanics of the mandible: A three-dimensional finite element study. *J. Biomech.* 1992;25(3):261-286.
98. Van Oosterwyck H, Duyck J, Vander Sloten J, et al. The influence of bone mechanical properties and implant fixation upon bone loading around oral implants. *Clin. Oral Implants Res.* 1998;9(6):407-418.
99. Palmquist A, Engqvist H, Lausmaa J, Thomsen P. Commercially Available Dental Implants: Review of Their Surface Characteristics. *Journal of Biomaterials and Tissue Engineering.* 2012;2(2):112-124.
100. Albrektsson T, Wennerberg A. Oral implant surfaces: Part 1--review focusing on topographic and chemical properties of different surfaces and in vivo responses to them. *Int. J. Prosthodont.* 2004;17(5):536-543.
101. Albrektsson T, Wennerberg A. Oral implant surfaces: Part 2--review focusing on clinical knowledge of different surfaces. *Int. J. Prosthodont.* 2004;17(5):544-564.
102. Junker R, Dimakis A, Thoneick M, Jansen JA. Effects of implant surface coatings and composition on bone integration: a systematic review. *Clin. Oral Implants Res.* 2009;20(s4):185-206.
103. Hagberg K, Branemark R. One hundred patients treated with osseointegrated transfemoral amputation prostheses--rehabilitation perspective. *J. Rehabil. Res. Dev.* 2009;46(3):331-344.
104. Branemark R, Branemark PI, Rydevik B, Myers RR. Osseointegration in skeletal reconstruction and rehabilitation: a review. *J. Rehabil. Res. Dev.* 2001;38(2):175-181.

105. Hagberg K, Branemark R, Gunterberg B, Rydevik B. Osseointegrated trans-femoral amputation prostheses: prospective results of general and condition-specific quality of life in 18 patients at 2-year follow-up. *Prosthet. Orthot. Int.* 2008;32(1):29-41.
106. Hagberg K, Haggstrom E, Uden M, Branemark R. Socket versus bone-anchored trans-femoral prostheses: hip range of motion and sitting comfort. *Prosthet. Orthot. Int.* 2005;29(2):153-163.
107. Lee WC, Frossard LA, Hagberg K, et al. Kinetics of transfemoral amputees with osseointegrated fixation performing common activities of daily living. *Clin. Biomech.* 2007;22(6):665-673.
108. Haggstrom E, Hagberg K, Rydevik B, Branemark R. Vibrotactile evaluation: osseointegrated versus socket-suspended transfemoral prostheses. *J. Rehabil. Res. Dev.* 2013;50(10):1423-1434.
109. Brånemark K-MHP-I. Immunohistochemical Study Of Clinical Skin-Penetrating Titanium Implants For Orthopaedic Prostheses Compared With Implants In The Craniofacial Area. *Scand. J. Plast. Reconstr. Surg. Hand Surg.* 2001;35(2):141-148.
110. Tillander J, Hagberg K, Hagberg L, Branemark R. Osseointegrated titanium implants for limb prostheses attachments: infectious complications. *Clin. Orthop. Relat. Res.* 2010;468(10):2781-2788.
111. Nebergall A, Bragdon C, Antonellis A, Karrholm J, Branemark R, Malchau H. Stable fixation of an osseointegated implant system for above-the-knee amputees: titel RSA and radiographic evaluation of migration and bone remodeling in 55 cases. *Acta Orthop.* 2012;83(2):121-128.
112. Xu W, Robinson K. X-ray image review of the bone remodeling around an osseointegrated trans-femoral implant and a finite element simulation case study. *Ann. Biomed. Eng.* 2008;36(3):435-443.
113. Hurkmans HLP, Bussmann JBJ, Benda E, Verhaar JAN, Stam HJ. Techniques for measuring weight bearing during standing and walking. *Clin. Biomech.* 2003;18(7):576-589.
114. Koehler SR, Dhaher YY, Hansen AH. Cross-validation of a portable, six-degree-of-freedom load cell for use in lower-limb prosthetics research. *J. Biomech.* 2014;47(6):1542-1547.
115. Lee WC, Frossard LA, Hagberg K, et al. Magnitude and variability of loading on the osseointegrated implant of transfemoral amputees during walking. *Med. Eng. Phys.* 2008;30(7):825-833.
116. Frossard L, Haggstrom E, Hagberg K, Branemark R. Load applied on bone-anchored transfemoral prosthesis: characterization of a prosthesis-a pilot study. *J. Rehabil. Res. Dev.* 2013;50(5):619-634.
117. D'Angeli V, Belvedere C, Ortolani M, Giannini S, Leardini A. Load along the femur shaft during activities of daily living. *J. Biomech.* 2013;46(12):2002-2010.
118. Lee WC, Doocey JM, Branemark R, et al. FE stress analysis of the interface between the bone and an osseointegrated implant for amputees--implications to refine the rehabilitation program. *Clin. Biomech.* 2008;23(10):1243-1250.
119. Prendergast PJ. Finite element models in tissue mechanics and orthopaedic implant design. *Clin. Biomech.* 1997;12(6):343-366.

120. Newcombe L, Dewar M, Blunn GW, Fromme P. Effect of amputation level on the stress transferred to the femur by an artificial limb directly attached to the bone. *Med. Eng. Phys.* 2013;35(12):1744-1753.
121. Tomaszewski PK, Verdonschot N, Bulstra SK, Rietman JS, Verkerke GJ. Simulated bone remodeling around two types of osseointegrated implants for direct fixation of upper-leg prostheses. *J. Mech. Behav. Biomed. Mater.* 2012;15:167-175.
122. Tomaszewski PK, Verdonschot N, Bulstra SK, Verkerke GJ. A Comparative Finite-Element Analysis of Bone Failure and Load Transfer of Osseointegrated Prostheses Fixations. *Ann. Biomed. Eng.* 2010;38(7):2418-2427.
123. Yerneni S, Dhaher Y, Kuiken TA. A computational model for stress reduction at the skin-implant interface of osseointegrated prostheses. *J. Biomed. Mater. Res. A.* 2012;100(4):911-917.
124. Sennerby L, Meredith N. Implant stability measurements using resonance frequency analysis: biological and biomechanical aspects and clinical implications. *Periodontol. 2000.* 2008;47:51-66.
125. Atsumi M, Park SH, Wang HL. Methods used to assess implant stability: current status. *Int. J. Oral Maxillofac. Implants.* 2007;22(5):743-754.
126. Brånemark R. *A biomechanical study of osseointegration : in-vivo measurements in rat, rabbit, dog and man.* Department of Orthopaedics, Institute of Surgical Sciences and Institute of Anatomy and Cell Biology, Göteborg University, Göteborg 1996.
127. Branemark R, Ohrnell LO, Nilsson P, Thomsen P. Biomechanical characterization of osseointegration during healing: an experimental in vivo study in the rat. *Biomaterials.* 1997;18(14):969-978.
128. Branemark R, Ohrnell LO, Skalak R, Carlsson L, Branemark PI. Biomechanical characterization of osseointegration: an experimental in vivo investigation in the beagle dog. *J. Orthop. Res.* 1998;16(1):61-69.
129. Doblaré M, García JM, Gómez MJ. Modelling bone tissue fracture and healing: a review. *Engineering Fracture Mechanics.* 2004;71(13–14):1809-1840.
130. Van Staden RC, Guan H, Loo YC. Application of the finite element method in dental implant research. *Comput. Methods Biomech. Biomed. Engin.* 2006;9(4):257-270.
131. Geng JP, Tan KB, Liu GR. Application of finite element analysis in implant dentistry: a review of the literature. *J. Prosthet. Dent.* 2001;85(6):585-598.
132. Huiskes R, Chao EYS. A survey of finite element analysis in orthopedic biomechanics: The first decade. *J. Biomech.* 1983;16(6):385-409.
133. Hansson S. Implant-abutment interface: biomechanical study of flat top versus conical. *Clin. Implant Dent. Relat. Res.* 2000;2(1):33-41.
134. Hansson S. A conical implant-abutment interface at the level of the marginal bone improves the distribution of stresses in the supporting bone. An axisymmetric finite element analysis. *Clin. Oral Implants Res.* 2003;14(3):286-293.

135. Simmons CA, Meguid SA, Pilliar RM. Differences in osseointegration rate due to implant surface geometry can be explained by local tissue strains. *J. Orthop. Res.* 2001;19(2):187-194.
136. Savadi RC, Agarwal J, Agarwal RS, Rangarajan V. Influence of Implant Surface Topography and Loading Condition on Stress Distribution in Bone Around Implants: A Comparative 3D FEA. *The Journal of the Indian Prosthodontic Society.* 2011;11(4):221-231.
137. Skalak R. Biomechanical considerations in osseointegrated prostheses. *J. Prosthet. Dent.* 1983;49(6):843-848.
138. Hansson S, Werke M. The implant thread as a retention element in cortical bone: the effect of thread size and thread profile: a finite element study. *J. Biomech.* 2003;36(9):1247-1258.
139. Simon U, Augat P, Ignatius A, Claes L. Influence of the stiffness of bone defect implants on the mechanical conditions at the interface--a finite element analysis with contact. *J. Biomech.* 2003;36(8):1079-1086.
140. Thelen S, Barthelat F, Brinson LC. Mechanics considerations for microporous titanium as an orthopedic implant material. *J. Biomed. Mater. Res. A.* 2004;69(4):601-610.
141. Dos Santos MV, Elias CN, Cavalcanti Lima JH. The Effects of Superficial Roughness and Design on the Primary Stability of Dental Implants. *Clin. Implant Dent. Relat. Res.* 2011;13(3):215-223.
142. Osullivan D, Sennerby L, Meredith N, et al. Influence of implant taper on the primary and secondary stability of osseointegrated titanium implants. *Clin. Oral Implants Res.* 2004;15(4):474-480.
143. Coelho PG, Granato R, Marin C, et al. The effect of different implant macrogeometries and surface treatment in early biomechanical fixation: An experimental study in dogs. *J. Mech. Behav. Biomed. Mater.* 2011;4(8):1974-1981.
144. Ivanoff CJ, Sennerby L, Johansson C, Rangert B, Lekholm U. Influence of implant diameters on the integration of screw implants. An experimental study in rabbits. *Int. J. Oral Maxillofac. Surg.* 1997;26(2):141-148.
145. de Vasconcellos LM, Oliveira FN, Leite Dde O, et al. Novel production method of porous surface Ti samples for biomedical application. *J. Mater. Sci. Mater. Med.* 2012;23(2):357-364.
146. Braem A, Chaudhari A, Vivan Cardoso M, Schrooten J, Duyck J, Vleugels J. Peri- and intra-implant bone response to microporous Ti coatings with surface modification. *Acta Biomater.* 2014;10(2):986-995.
147. Tabassum A, Meijer GJ, Wolke JG, Jansen JA. Influence of the surgical technique and surface roughness on the primary stability of an implant in artificial bone with a density equivalent to maxillary bone: a laboratory study. *Clin. Oral Implants Res.* 2009;20(4):327-332.
148. Shalabi MM, Wolke JG, Jansen JA. The effects of implant surface roughness and surgical technique on implant fixation in an in vitro model. *Clin. Oral Implants Res.* 2006;17(2):172-178.

149. Turkyilmaz I, Aksoy U, McGlumphy EA. Two alternative surgical techniques for enhancing primary implant stability in the posterior maxilla: a clinical study including bone density, insertion torque, and resonance frequency analysis data. *Clin. Implant Dent. Relat. Res.* 2008;10(4):231-237.
150. van Staden RC, Guan H, Johnson NW, Loo YC, Meredith N. Step-wise analysis of the dental implant insertion process using the finite element technique. *Clin. Oral Implants Res.* 2008;19(3):303-313.
151. Trisi P, Todisco M, Consolo U, Travaglini D. High versus low implant insertion torque: a histologic, histomorphometric, and biomechanical study in the sheep mandible. *The International journal of oral & maxillofacial implants.* 2011;26(4):837-849.
152. Trisi P, Perfetti G, Baldoni E, Berardi D, Colagiovanni M, Scogna G. Implant micromotion is related to peak insertion torque and bone density. *Clin. Oral Implants Res.* 2009;20(5):467-471.
153. Molly L. Bone density and primary stability in implant therapy. *Clin. Oral Implants Res.* 2006;17 Suppl 2:124-135.
154. Turkyilmaz I, McGlumphy E. Influence of bone density on implant stability parameters and implant success: a retrospective clinical study. *BMC Oral Health.* 2008;8(1):32.
155. Papavasiliou G, Kamposiora P, Bayne SC, Felton DA. 3D-FEA of osseointegration percentages and patterns on implant-bone interfacial stresses. *J. Dent.* 1997;25(6):485-491.
156. Gadelmawla ES, Koura MM, Maksoud TMA, Elewa IM, Soliman HM. Roughness parameters. *Journal of Materials Processing Technology.* 2002;123:133-145.
157. Hansson S. Surface roughness parameters as predictors of anchorage strength in bone: a critical analysis. *J. Biomech.* 2000;33(10):1297-1303.
158. Hansson S, Norton M. The relation between surface roughness and interfacial shear strength for bone-anchored implants. A mathematical model. *J. Biomech.* 1999;32(8):829-836.
159. Hansson S, Löberg J, Mattisson I, Ahlberg E. Characterisation of Titanium Dental Implants. II: Local Biomechanical Model. *The Open Biomaterials Journal.* 2010;2:36-52.
160. Hansson S, Löberg J, Mattisson I, Ahlberg E. Global biomechanical model for dental implants. *J. Biomech.* 2011;44(6):1059-1065.
161. Stenlund P, Murase K, Stalhandske C, Lausmaa J, Palmquist A. Understanding mechanisms and factors related to implant fixation; a model study of removal torque. *J. Mech. Behav. Biomed. Mater.* 2014;34C:83-92.
162. Shalabi MM, Gortemaker A, Van't Hof MA, Jansen JA, Creugers NH. Implant surface roughness and bone healing: a systematic review. *J. Dent. Res.* 2006;85(6):496-500.
163. Buser D, Schenk RK, Steinemann S, Fiorellini JP, Fox CH, Stich H. Influence of surface characteristics on bone integration of titanium implants. A histomorphometric study in miniature pigs. *J. Biomed. Mater. Res.* 1991;25(7):889.
164. Butz F, Aita H, Wang CJ, Ogawa T. Harder and stiffer bone osseointegrated to roughened titanium. *J. Dent. Res.* 2006;85(6):560-565.

165. Yeo I-S, Han J-S, Yang J-H. Biomechanical and histomorphometric study of dental implants with different surface characteristics. *Journal of biomedical materials research.Part B, Applied biomaterials.* 2008;87(2):303-311.
166. Wennerberg A, Ektessabi A, Albrektsson T, Johansson C, Andersson B. A 1-year follow-up of implants of differing surface roughness placed in rabbit bone. *Int. J. Oral Maxillofac. Implants.* 1997;12(4):486-494.
167. Elias CN, Oshida Y, Lima JHC, Muller CA. Relationship between surface properties (roughness, wettability and morphology) of titanium and dental implant removal torque. *J. Mech. Behav. Biomed. Mater.* 2008;1(3):234-242.
168. Wennerberg A, Albrektsson T, Lausmaa J. Torque and histomorphometric evaluation of c.p. titanium screws blasted with 25- and 75-microns-sized particles of Al2O3. *J. Biomed. Mater. Res.* 1996;30(2):251-260.
169. Branemark R, Emanuelsson L, Palmquist A, Thomsen P. Bone response to laser-induced micro- and nano-size titanium surface features. *Nanomed.* 2011;7(2):220-227.
170. Palmquist A, Emanuelsson L, Branemark R, Thomsen P. Biomechanical, histological and ultrastructural analyses of laser micro- and nano-structured titanium implant after 6 months in rabbit. *J. Biomed. Mater. Res. B Appl. Biomater.* 2011;97(2):289-298.
171. Klokkevold PR, Johnson P, Dadgostari S, Davies JE, Caputo A, Nishimura RD. Early endosseous integration enhanced by dual acid etching of titanium: a torque removal study in the rabbit. *Clin. Oral Implants Res.* 2001;12(4):350-357.
172. Johansson CB, Gretzer C, Jimbo R, Mattisson I, Ahlberg E. Enhanced implant integration with hierarchically structured implants: a pilot study in rabbits. *Clin. Oral Implants Res.* 2012;23(8):943-953.
173. Coelho PG, Bonfante EA, Pessoa RS, et al. Characterization of five different implant surfaces and their effect on osseointegration: a study in dogs. *J. Periodontol.* 2011;82(5):742-750.
174. Coelho PG, Granato R, Marin C, et al. Biomechanical evaluation of endosseous implants at early implantation times: a study in dogs. *J. Oral Maxillofac. Surg.* 2010;68(7):1667-1675.
175. Murr LE, Gaytan SM, Martinez E, Medina F, Wicker RB. Next generation orthopaedic implants by additive manufacturing using electron beam melting. *International journal of biomaterials.* 2012;2012:245727.
176. de Peppo GM, Palmquist A, Borchardt P, et al. Free-form-fabricated commercially pure Ti and Ti6Al4V porous scaffolds support the growth of human embryonic stem cell-derived mesodermal progenitors. *ScientificWorldJournal.* 2012;2012:646417.
177. Hrabe NW, Heinl P, Bordia RK, Korner C, Fernandes RJ. Maintenance of a bone collagen phenotype by osteoblast-like cells in 3D periodic porous titanium (Ti-6Al-4 V) structures fabricated by selective electron beam melting. *Connect. Tissue Res.* 2013;54(6):351-360.
178. Thomsen P, Malmstrom J, Emanuelsson L, Rene M, Snis A. Electron beam-melted, free-form-fabricated titanium alloy implants: Material surface characterization and early bone response in rabbits. *J. Biomed. Mater. Res. B Appl. Biomater.* 2009;90(1):35-44.

179. Palmquist A, Snis A, Emanuelsson L, Browne M, Thomsen P. Long-term biocompatibility and osseointegration of electron beam melted, free-form-fabricated solid and porous titanium alloy: Experimental studies in sheep. *J. Biomater. Appl.* 2013;27(8):1003-1016.
180. Stenlund P, Kurosu S, Koizumi Y, et al. Osseointegration Enhancement by Zr doping of Co-Cr-Mo Implants Fabricated by Electron Beam Melting. *Additive Manufacturing.* 2015;6(0):6-15.
181. Engh CA, Bobyn JD, Glassman AH. Porous-Coated Hip-Replacement - the Factors Governing Bone Ingrowth, Stress Shielding, and Clinical-Results. *Journal of Bone and Joint Surgery-British Volume.* 1987;69(1):45-55.
182. Sotereanos NG, Engh CA, Glassman AH, Macalino GE, Engh CA, Jr. Cementless femoral components should be made from cobalt chrome. *Clin. Orthop. Relat. Res.* 1995(313):146-153.
183. Wennerberg A, Albrektsson T. Effects of titanium surface topography on bone integration: a systematic review. *Clin. Oral Implants Res.* 2009;20 Suppl 4:172-184.
184. Mendonca G, Mendonca DB, Aragao FJ, Cooper LF. Advancing dental implant surface technology--from micron- to nanotopography. *Biomaterials.* 2008;29(28):3822-3835.
185. Le Guehennec L, Soueidan A, Layrolle P, Amouriq Y. Surface treatments of titanium dental implants for rapid osseointegration. *Dent. Mater.* 2007;23(7):844-854.
186. Wen X, Wang X, Zhang N. Microrough surface of metallic biomaterials: a literature review. *Biomed. Mater. Eng.* 1996;6(3):173-189.
187. Kasemo B, Lausmaa J. Biomaterial and implant surfaces: on the role of cleanliness, contamination, and preparation procedures. *J. Biomed. Mater. Res.* 1988;22(A2 Suppl):145-158.
188. Eisenbarth E, Velten D, Müller M, Thull R, Breme J. Biocompatibility of β-stabilizing elements of titanium alloys. *Biomaterials.* 2004;25(26):5705-5713.
189. Stenport VF, Johansson CB. Evaluations of bone tissue integration to pure and alloyed titanium implants. *Clin. Implant Dent. Relat. Res.* 2008;10(3):191-199.
190. Stenlund P, Omar O, Brohede U, et al. Bone response to a novel Ti-Ta-Nb-Zr alloy. *Acta Biomater.* 2015, (In press) http://dx.doi.org/10.1016/j.actbio.2015.03.038
191. Sul Y-T, Johansson C, Albrektsson T, Örebro u, Institutionen för klinisk m. Which surface properties enhance bone response to implants? Comparison of oxidized magnesium, TiUnite, and Osseotite implant surfaces. *The International journal of prosthodontics.* 2006;19(4):319.
192. Wen B, Zhu F, Li Z, Zhang P, Lin X, Dard M. The osseointegration behavior of titanium-zirconium implants in ovariectomized rabbits. *Clin. Oral Implants Res.* 2014;25(7):819-825.
193. Sul YT, Johansson C, Wennerberg P, Cho LR, Chang BS, Albrektsson P. Optimum surface properties of oxidized implants for reinforcement of osseointegration: Surface chemistry, oxide thickness, porosity, roughness, and crystal structure. *Int. J. Oral Maxillofac. Implants.* 2005;20(3):349-359.

194. Thomsen P, Larsson C, Ericson LE, Sennerby L, Lausmaa J, Kasemo B. Structure of the interface between rabbit cortical bone and implants of gold, zirconium and titanium. *J. Mater. Sci. Mater. Med.* 1997;8(11):653-665.
195. Johansson C, Lausmaa J, Ask M, Hansson HA, Albrektsson T. Ultrastructural differences of the interface zone between bone and Ti 6Al 4V or commercially pure titanium. *J. Biomed. Eng.* 1989;11(1):3-8.
196. Hoerth RM, Katunar MR, Gomez Sanchez A, et al. A comparative study of zirconium and titanium implants in rat: osseointegration and bone material quality. *J. Mater. Sci.: Mater. Med.* 2014;25(2):411-422.
197. Jakobsen SS, Baas J, Jakobsen T, Soballe K. Biomechanical implant fixation of CoCrMo coating inferior to titanium coating in a canine implant model. *J. Biomed. Mater. Res. A.* 2010;94(1):180-186.
198. Jinno T, Goldberg VM, Davy D, Stevenson S. Osseointegration of surface-blasted implants made of titanium alloy and cobalt-chromium alloy in a rabbit intramedullary model. *J. Biomed. Mater. Res.* 1998;42(1):20-29.
199. Nanci A, Wuest JD, Peru L, et al. Chemical modification of titanium surfaces for covalent attachment of biological molecules. *J. Biomed. Mater. Res.* 1998;40(2):324-335.
200. Cooper LF. Biologic determinants of bone formation for osseointegration: Clues for future clinical improvements. *The Journal of prosthetic dentistry.* 1998;80(4):439-449.
201. Willie BM, Yang X, Kelly NH, et al. Cancellous Bone Osseointegration Is Enhanced by In Vivo Loading. *Tissue Eng Part C Methods.* 2010;16(6):1399-1406.
202. Hoshaw S, Brunski J, Cochran G. Mechanical Loading of Brånemark Implants Affects Interfacial Bone Modeling and Remodeling. *The international journal of oral & maxillofacial implants.* 1994;9(3):345-360.
203. Romanos GE, Toh CG, Siar CH, Wicht H, Yacoob H, Nentwig G-H. Bone-implant interface around titanium implants under different loading conditions: a histomorphometrical analysis in the Macaca fascicularis monkey. *J. Periodontol.* 2003;74(10):1483-1490.
204. Brunski JB. In vivo bone response to biomechanical loading at the bone/dental-implant interface. *Adv. Dent. Res.* 1999;13:99-119.
205. Torcasio A, van Lenthe GH, Van Oosterwyck H. The importance of loading frequency, rate and vibration for enhancing bone adaptation and implant osseointegration. *Eur. Cell. Mater.* 2008;16:56-68.
206. Isidor F. Influence of forces on peri-implant bone. *Clin. Oral Implants Res.* 2006;17(S2):8-18.
207. Wiskott HW, Belser UC. Lack of integration of smooth titanium surfaces: a working hypothesis based on strains generated in the surrounding bone. *Clin. Oral Implants Res.* 1999;10(6):429-444.
208. Lausmaa J. Mechanical, Thermal, Chemical and Electrochemical Surface Treatment of Titanium. *Titanium in Medicine*: Springer Berlin Heidelberg; 2001:231-266.
209. ISO 10993-5:2009 Biological evaluation of medical devices — Part 5: Tests for in vitro cytotoxicity.

210. ISO 10993-5:2009 Biological evaluation of medical devices — Part 12: Sample preparation and reference materials.
211. Branemark R, Skalak R. An in-vivo method for biomechanical characterization of bone-anchored implants. *Med. Eng. Phys.* 1998;20(3):216-219.
212. Regis M, Marin E, Fedrizzi L, Pressacco M. Additive manufacturing of Trabecular Titanium orthopedic implants. *MRS Bulletin.* 2015;40(2):137.
213. Glon F, Flys O, Loof PJ, Rosen BG. 3D SEM for surface topography quantification - a case study on dental surfaces. *J Phys Conf Ser.* 2014;483.
214. Stout KJ, Sullivan PJ, Dong WP, et al. *The Development of Methods for the Characterisation of Roughness in Three Dimensions.* Report EUR 15178 EN (European Commision, Brussels 1993).
215. Wennerberg A, Albrektsson T. Suggested guidelines for the topographic evaluation of implant surfaces. *Int. J. Oral Maxillofac. Implants.* 2000;15(3):331-344.
216. Lennerås M, Palmquist A, Norlindh B, Emanuelsson L, Thomsen P, Omar O. Oxidized Titanium Implants Enhance Osseointegration via Mechanisms Involving RANK/RANKL/OPG Regulation. *Clin. Implant Dent. Relat. Res.* 2014;Dec 23 [Epub ahead of print].
217. Morais LS, Serra GG, Muller CA, et al. Titanium alloy mini-implants for orthodontic anchorage: immediate loading and metal ion release. *Acta Biomater.* 2007;3(3):331-339.
218. Matsuno H, Yokoyama A, Watari F, Uo M, Kawasaki T. Biocompatibility and osteogenesis of refractory metal implants, titanium, hafnium, niobium, tantalum and rhenium. *Biomaterials.* 2001;22(11):1253-1262.
219. Okazaki Y, Gotoh E. Comparison of metal release from various metallic biomaterials in vitro. *Biomaterials.* 2005;26(1):11-21.
220. Okazaki Y, Gotoh E, Nishimori M, Katsuda S-i, Manabe T, Kobayashi K. Osteocompatibility of Stainless Steel, Co–Cr–Mo, Ti–6Al–4V and Ti–15Zr–4Nb–4Ta Alloy Implants in Rat Bone Tissue. *Mater. Trans.* 2005;46(7):1610-1617.
221. Challa VSA, Mali S, Misra RDK. Reduced toxicity and superior cellular response of preosteoblasts to Ti-6Al-7Nb alloy and comparison with Ti-6Al-4V. *J. Biomed. Mater. Res., Part A.* 2013;101A(7):2083-2089.
222. Rogers SD, Howie DW, Graves SE, Pearcy MJ, Haynes DR. In vitro human monocyte response to wear particles of titanium alloy containing vanadium or niobium. *J. Bone Joint Surg. Br.* 1997;79B(2):311-315.
223. Grandin HM, Berner S, Dard M. A Review of Titanium Zirconium (TiZr) Alloys for Use in Endosseous Dental Implants. *Materials.* 2012;5(8):1348-1360.
224. Pourbaix M. *Atlas of electrochemical equilibria in aqueous solutions.* National Association of Corrosion Engineers; 1974.
225. Numata Y, Syuto B, Nomura N, Chiba A. Cytocompatibility for Co-Cr-Mo alloy with a small amount of zirconium or carbon. *Journal of Japan Institute of Metals.* 2007;71(7):578-585.

226. Kurosu S, Nomura N, Yamaguchi K, Fujinuma S, Chiba A. Effects of 5th Element Addition to Co-29Cr-6Mo Alloy Containing Impurity Ni on Metal Ion Release. *Journal of Japan Institute of Metals.* 2005;69(10):886-891.
227. Behl B, Papageorgiou I, Brown C, et al. Biological effects of cobalt-chromium nanoparticles and ions on dural fibroblasts and dural epithelial cells. *Biomaterials.* 2013;34(14):3547-3558.
228. Omar OM, Lenneras ME, Suska F, et al. The correlation between gene expression of proinflammatory markers and bone formation during osseointegration with titanium implants. *Biomaterials.* 2011;32(2):374-386.
229. Löberg J, Mattisson I, Hansson S, Ahlberg E. Characterisation of Titanium Dental Implants I: Critical Assessment of Surface Roughness. *The Open Biomaterials Journal.* 2010;2:18-35.
230. Gupta HS, Zioupos P. Fracture of bone tissue: The 'hows' and the 'whys'. *Med. Eng. Phys.* 2008;30(10):1209-1226.
231. Li J, Liao H, Fartash B, Hermansson L, Johnsson T. Surface-dimpled commercially pure titanium implant and bone ingrowth. *Biomaterials.* 1997;18(9):691-696.
232. Götz HE, Müller M, Emmel A, Holzwarth U, Erben RG, Stangl R. Effect of surface finish on the osseointegration of laser-treated titanium alloy implants. *Biomaterials.* 2004;25(18):4057-4064.
233. Stangl R, Pries A, Loos B, Müller M, Erben RG. Influence of pores created by laser superfinishing on osseointegration of titanium alloy implants. *Journal of biomedical materials research.Part A.* 2004;69(3):444.
234. Skerry TM. Mechanical loading and bone: What sort of exercise is beneficial to the skeleton? *Bone.* 1997;20(3):179-181.
235. Halldin A, Jimbo R, Johansson CB, et al. The effect of static bone strain on implant stability and bone remodeling. *Bone.* 2011;49(4):783-789.
236. Halldin A, Jimbo R, Johansson CB, et al. Implant Stability and Bone Remodeling after 3 and 13 Days of Implantation with an Initial Static Strain. *Clin. Implant Dent. Relat. Res.* 2014;16(3):383-393.
237. Bashutski JD, D'Silva NJ, Wang H-L. Implant compression necrosis: current understanding and case report. *J. Periodontol.* 2009;80(4):700-704.
238. Rubin CT, Lanyon LE. Regulation of bone formation by applied dynamic loads. *J. Bone Joint Surg. Am.* 1984;66(3):397-402.